

Low-energy electron scattering from CO. II. *Ab initio* study using the frame-transformation theory

N. Chandra*†

Theoretical Studies Group, National Aeronautics and Space Administration, Goddard Space Flight Center, Greenbelt, Maryland 20771

(Received 28 June 1976; revised manuscript received 3 February 1977)

The frame-transformation theory has been employed to extend first-principles studies of electron-molecule collisions to heteronuclear diatomic systems. The Wigner-Eisenbud R matrix has been introduced at the boundary point of the molecular-core radius—which defines the inner region—in a molecule-fixed frame of reference in the fixed-nuclei approximation. The solutions of the scattering equations in the outer region, where rotational motion of the nuclei is taken into account, are continued by transforming the R matrix to the space frame of reference. This procedure has been applied to a model calculation of thermal-energy electron scattering from CO. The dependence of the rotational transition cross sections on the core radius has been studied. A general methodology has been developed for adapting the single-center pseudopotential method to the proposed amalgamation of the R -matrix and frame-transformation theories in order to perform a fundamental calculation of the interior problem. A comprehensive study of e^- -CO scattering is carried out on the basis of this methodology. In the present application the dipole term in the multipole expansion of the static potential, computed from the ground-electronic state wave functions of the CO molecule, has been renormalized so that it reproduces, asymptotically, the experimentally measured magnitude of the dipole moment of carbon monoxide. The calculated momentum-transfer cross section is in good agreement with the experimental measurements for thermal-energy e^- scattering from CO. The rotational excitation and deexcitation, and total scattering and momentum-transfer cross sections computed from this method also reproduce the 1.75 eV $^2\Pi$ resonance; while those obtained from an extension of the model calculation mentioned above fail to do so. In particular, it is found that for rotationally inelastic scattering in the resonance region the cross sections for $0 \rightarrow 4$ and $1 \rightarrow 3$ transitions are the largest among those which start from the ground and first rotational states of CO molecule, respectively. The angular distributions for various electron impact transitions in CO have also been computed.

I. INTRODUCTION

The absence of a center of symmetry in heteronuclear diatomic molecules, which also gives rise to a nonvanishing permanent dipole moment, makes it more difficult, physically as well as numerically, to study electron scattering from polar-molecular targets compared to that from homonuclear systems. It has been shown in a recent communication¹ (hereafter referred to as I) that for electron scattering in a frame of reference attached to the molecule (i.e., the molecular-frame or the body-frame of reference) the single-center expansions of the bound and continuum molecular orbitals converge very well even for complex targets, albeit at a slow rate for low-symmetry systems.

For heteronuclear molecules this problem of slow convergence is compounded by the fact that because of the presence of a long-range r^{-2} electron-dipole interaction potential the phase shift for higher angular momenta behaves¹ as $l^{-1/2}$ for electron scattering from a fixed polar molecule in body frame of reference. As a result, the total scattering cross section, averaged over all molecular orientations, diverges logarithmically¹ in the fixed-nuclei approximation.² (However, as proved in I, the momentum transfer cross

section is finite even in this approximation.) The fact that the time-averaged field of a rotating dipole is zero makes it necessary that in order to obtain finite total cross section the rotational motion of the nuclei should be included in the equations for scattering of an electron from a polar molecule.

Amongst the existing theoretical formulations of electron-molecule collisions, the use of the fundamental theory of Arthurs and Dalgarno³ for scattering of a structureless particle from a rigid rotor makes a natural choice to study the electron-polar molecule scattering. This space (lab)-frame formulation of the collision problem retains the rotational kinetic energy terms in the total Hamiltonian of the (electron+molecule) system.

There have been several attempts to apply this theory to electron scattering from various polar-molecular targets.⁴ Almost all of these studies are, however, phenomenological in nature based upon some *ad hoc* semiempirical potentials where no account has been taken to represent the highly anisotropic short-range terms and the exchange effects of the electron-molecule interaction in the scattering equations. However, it has been found that even for such simple system as H_2 , where the short-range terms are not so noncentral

and strong, it is extremely difficult to carry out the expansion in $(v)jl$ basis channels to complete convergence limit.^{2,5} Therefore, the application of this theory to electron scattering from more complex systems with an emphasis to represent the nuclear singularities and the exchange effects in the scattering equations as accurately as possible and in a nonphenomenological way will become almost impossible numerically.

Although the expansion of the total wave function in l , which forms the only basis channel for electron scattering in a body frame of reference in fixed-nuclei approximation, does converge very well, but the fact that the total cross section for scattering from polar molecules in this approximation is not finite¹ also excludes the possibility of using the adiabatic-nuclei theory² to calculate vibration-rotation excitation cross sections for electron-heteronuclear-molecule collisions.

The natural question which one should ask now is: Is it physically valid to perform the Born-Oppenheimer separation of the electronic and nuclear motions at some stage in the electron-molecule collision process? The well-known answer to this question lies in the fact that, whether in any part of the whole scattering region, the duration of collision is smaller than the time period for vibration and/or rotation of the nuclei. When the electron is far away from the molecular core, where the nuclear singularities are not so effective and the short-range and exchange terms have almost vanished, the slow motion of the electron compared to the vibration rotation will certainly cause the Born-Oppenheimer approximation to break down. In this outer region, therefore, one will have to include the nuclear kinetic energy terms in the scattering equations.

The validity of the Born-Oppenheimer approximation in the inner-molecule core region is, however, a much more involved question. A naive reasoning based upon the observation that an increase in the incident electron's velocity due to strong attractive short-range forces will cause the electron to move faster in this region than the vibrating-rotating nuclei will lead to the conclusion that the separation of the electronic and nuclear motions will always be valid in the inner region. However, as recently discovered by Chandra and Temkin⁶ in their study of vibrational excitation in e^- - N_2 scattering and previously discussed by Herzenberg⁷ for other molecular systems, a trapping of the incident electron in the noncentral molecular field—which is a combination of the centrifugal barrier, permanent moments, and the induced dipole polarizability—may always enhance the transition time, such that before the

incident electron becomes free again the molecular nuclei are able to change their configuration. Under these circumstances one can certainly not neglect the effects of the nuclear motion relative to that of the incident electron. Therefore, the validity of the Born-Oppenheimer approximation in the molecular-core region is not always a predetermined fact.

When the separation of the motions of the incident electron and the nuclei in the molecular-core region is a viable approximation one can always neglect the nuclear vibration rotation in the inner part of the configuration space. These two different physical situations—where one uses a fixed-nuclei approximation in the inner region and consider the nuclear rotation in the outer region in a space-fixed frame of reference—have been combined by an orthogonal transformation operator at the common boundary point by Chang and Fano⁸ in their frame-transformation (FT) theory of electron-molecule scattering.

If the Born-Oppenheimer approximation is valid for electron collision with certain polar molecules in the core region then the FT theory will provide a natural framework for studying electron scattering from such target systems. A fixed-nuclei treatment in the inner region will make very convenient the inclusion of nuclear singularities and the exchange effects in the scattering equations. At the same time the introduction of the nuclear rotation in the scattering equations in the outer region will cause all the scattering cross sections to be finite which are otherwise undefined in fixed- and adiabatic-nuclei approximations. The convergence problem in the basis set (jl) in a lab frame in the outer region is not expected to be so severe now as the strong noncentral short-range interaction potential terms are almost negligible and it is only the long-range terms which will have to be considered.

Among the diatomic heteronuclear molecules, carbon monoxide is a case of particular interest. Apart from being important from a space and environmental point of view, high-energy CO lasers play a significant role in scientific applications. The electron-swarm data for CO molecule have yielded scattering cross sections over a considerable range of energy.⁹ Moreover, the time period for the rotational motion of carbon monoxide is larger than the duration of collision of an electron with this molecule. Being isoelectronic to N_2 , it has a closed-shell ground-electronic-state configuration. We have reported in I that the single-center pseudopotential method, originally introduced by Burke and Chandra¹⁰ in their fixed-nuclei study of e^- - N_2 scattering and recently proved to be extremely successful⁶ in

electron-impact vibrational excitation of nitrogen molecule, works very well even for electron scattering from CO.

In view of these considerations and in continuation of our efforts to study the electron-molecule collisions from first principles using *ab initio* methods,^{1,2,6,10,11} we have, therefore, employed the FT theory to study rotationally elastic and inelastic e^- -CO scattering. Earlier, Chandra and Gianturco¹² gave a brief description of the methodology of applying the FT theory to study electron-molecule scattering in general and e^- -CO scattering in particular. (Note that the results of this letter with regard to CO are no longer valid because of an error discovered later and discussed in detail in I.) Short reports on the progress of the present work have been given elsewhere.¹³

Section II is a review of the essential elements of the FT theory and the relevant formulas. Chang and Fano⁸ have suggested that the wave functions and their derivatives, obtained by solving the fixed-nuclei scattering equations in the inner region, should be transformed separately to a space-fixed frame of reference to continue the solution of the scattering equations in the outer region. In our methodology of implementing the FT theory we calculate the Wigner¹⁴ \underline{R} matrix at the boundary point by using the solutions and the derivatives of the fixed-nuclei equations in the inner region. This \underline{R} matrix is then transformed to the lab frame by applying the orthogonal transformation given by Chang and Fano.⁸ The computation of a body-frame \underline{R} matrix, its transformation to a space-fixed frame of reference, and then the subsequent matching to the solutions of the outer-region equations for calculating the \underline{S} matrix is discussed in Sec. III.

To our knowledge the present work shall constitute the very first application of the FT theory for studying the electron-molecule collisions. (Henry and Chang¹⁵ and Chang¹⁶ had tried to apply this theory to e^- -H₂ scattering. In their studies they have made an approximation by neglecting the solutions of the scattering equations in the outer region in the lab frame. In a recent communication, Chandra¹⁷ has shown that under this approximation the FT and the adiabatic-nuclei theories are equivalent. Therefore, the e^- -H₂ calculations of Refs. 15 and 16 essentially reduce to an application of the adiabatic-nuclei theory.) In order to carry out a complete FT treatment the numerical implementation of the procedure, briefly pointed out in the preceding paragraph, becomes a complex and arduous task. We, therefore, thought it to be extremely important to test this theory and develop a feeling about its

physics and the confidence in our numerical procedure by applying it first to a previously undertaken semiempirical calculation based upon some simple potential

The first part of Sec. IV describes in detail our test study of the application of the FT theory to a model calculation of thermal energy electron scattering from CO done by Crawford and Dalgarno¹⁸ and compares our new results with those of their rotational close-coupling calculations. The second part of Sec. IV discusses how the single-center pseudopotential method can be adapted to our methodology, the effect of different choices of the boundary point—defining the inner-molecular core region—where a transformation is performed from a molecule-fixed to a space-fixed frame of reference, and the convergence of the (jl) basis set in the outer region. The final differential and integrated cross sections for electron-impact rotational transitions in a CO molecule together with the total scattering and momentum transfer cross sections are also presented in Sec. IV. The concluding Sec. V briefly discusses, on the basis of our present experience, the usefulness of the FT theory in studying the electron-molecule collision in general and the electron-polar molecule scattering in particular.

II. THEORY

A. Electron scattering in a space-fixed frame of reference

The total Hamiltonian of the (electron + molecule) system can be written as (in a.u.)

$$-\frac{1}{2}\nabla_{\vec{r}}^2 + H_e(\vec{r}_1, \dots, \vec{r}_N; \vec{R}) + H_{\text{rot}}(\hat{R}) + V(\vec{r}_1, \dots, \vec{r}_N, \vec{r}; \vec{R}). \quad (2.1)$$

The Schrödinger equation,

$$H_e(\vec{r}_1, \dots, \vec{r}_N; \vec{R})\Phi_n(\vec{r}_1, \dots, \vec{r}_N; \vec{R}) = \epsilon_n(R)\Phi_n(\vec{r}_1, \dots, \vec{r}_N; \vec{R}), \quad (2.2)$$

describes the n th state of the motion of N electrons of the target molecule,

$$H_{\text{rot}}(\hat{R}) Y_{jm_j}(\hat{R}) = B j(j+1) Y_{jm_j}(\hat{R}), \quad (2.3)$$

is the eigenvalue equation for the rotation of the nuclei when the molecule is in its $^1\Sigma$ electronic state, and in Eq. (2.1) we do not consider the vibrational motion of the nuclei. In Eq. (2.3) the rotational constant $B = (2I)^{-1}$, where I is the moment of inertia of the molecule. The electron-molecule interaction energy is given by

$$V(\vec{r}'_1, \dots, \vec{r}'_N, \vec{r}'; \vec{R}) = \sum_{i=1}^N \frac{1}{|\vec{r}' - \vec{r}'_i|} - \left(\frac{Z_A}{|\vec{r}' - \vec{R}_A|} + \frac{Z_B}{|\vec{r}' - \vec{R}_B|} \right), \quad (2.4)$$

where Z_A and Z_B are the atomic charges of the two nuclei A and B separated by distances $|\vec{R}_A|$ and $|\vec{R}_B|$ from the center of mass of the molecule.

The total wave function

$$\Psi^{JM}(\vec{r}'_1, \dots, \vec{r}'_N, \vec{r}; \vec{R}) = \Phi_0(\vec{r}'_1, \dots, \vec{r}'_N; \vec{R}) r^{-1} \sum_{\substack{j'l'l' \\ m'_j m'_l}} (-1)^{l'-j'-m} \left(\frac{(2j'+1)(2l'+1)}{4\pi} \right)^{1/2} \\ \times \begin{pmatrix} j' & l' & J \\ m'_j & m'_l & -M \end{pmatrix} u_{j'l'}^{j'}(r) Y_{l'm'_l}(\hat{r}) D_{m'_j 0}^{j'}(\hat{R}) \quad (2.5)$$

for scattering in a space-fixed frame of reference with the Hamiltonian (2.1) will yield the following set of equations³

$$\left(\frac{d^2}{dr^2} - \frac{l(l+1)}{r^2} + k_j^2 \right) u_{jl}^j(r) = 2 \sum_{j'l'} \sum_{\mu} (-1)^{j'-\mu} [(2j+1)(2l+1)(2j'+1)(2l'+1)]^{1/2} \\ \times \begin{pmatrix} j & j' & \mu \\ 0 & 0 & 0 \end{pmatrix} \begin{pmatrix} l & l' & \mu \\ 0 & 0 & 0 \end{pmatrix} \left\{ \begin{matrix} j' & l' & J \\ l & j & \mu \end{matrix} \right\} V_{\mu}(r) u_{j'l'}^{j'}(r), \quad (2.6)$$

where

$$k_j^2 = 2[E_T - \epsilon_0 - B_j(j+1)] \quad (2.7)$$

with E_T as the total energy of the colliding particles. [The rotation matrices \underline{D} , used in Eq. (2.5), have been defined by Rose¹⁹ and for the definition of the $3-j$, $6-j$, etc. symbols see, for example, Rotenberg *et al.*²⁰] On the right-hand side of Eq. (2.6), we have also used the multipole expansion of the molecular charge distribution about the center of mass of the molecule,²¹ i.e.,

$$V(\vec{r}; \vec{R}) = \langle \Phi_0(\vec{r}'_1, \dots, \vec{r}'_N; \vec{R}) | V(\vec{r}'_1, \dots, \vec{r}'_N, \vec{r}; \vec{R}) | \Phi_0(\vec{r}'_1, \dots, \vec{r}'_N; \vec{R}) \rangle \\ = \sum_{\mu} V_{\mu}(r) P_{\mu}(\hat{r} \cdot \hat{R}). \quad (2.8)$$

The summation index μ will have both even and odd integral values for heteronuclear diatomic molecules like CO, but only even integral values for homonuclear systems.

The coupled Eqs. (2.6), which will split up into two different sets according to the parity $(-1)^{j+l}$ for the same value of J , are solved subject to the following boundary conditions

$$u_{j'l'}^{j'}(r) \underset{r \rightarrow 0}{\sim} 0 \\ \underset{r \rightarrow 0}{\sim} k_j^{-1/2} [\sin(k_j r - \frac{1}{2} l' \pi) \delta_{jj}, \delta_{ll'} + \cos(k_j r - \frac{1}{2} l' \pi) K_{j'l'}^{j'}] \text{ for } k_j^2 > 0 \\ \underset{r \rightarrow \infty}{\sim} |k_j|^{-1/2} \exp(-|k_j| r) \text{ for } k_j^2 < 0, \quad (2.9)$$

in order to calculate the scattering matrix

$$\underline{S}^J = (1 + i\underline{K}^J)(1 - i\underline{K}^J)^{-1} \quad (2.10)$$

and the transition matrix

$$\underline{T}^J = \underline{S}^J - 1 = 2i\underline{K}^J(1 - i\underline{K}^J)^{-1}. \quad (2.11)$$

The first set of (j', l') subscript on u^J in Eq. (2.9) refers to the outgoing channel while the second set (j, l) is for the incident channel.

The formulas for various cross sections for a transition from molecular rotational state j to j'

have been derived by Arthurs and Dalgarno in the original paper.³ However, these expressions can be further simplified²² by using the concept of angular momentum transfer, $\vec{l}_1 = \vec{j}' - \vec{j} = \vec{l} - \vec{l}'$ (where $\vec{J} = \vec{j} + \vec{l} = \vec{j}' + \vec{l}'$), introduced by Fano and Dill.²³ In this simplified form, the differential cross section for $(j-j')$ transition becomes²²

$$\frac{d\sigma_{j-j'}}{d\Omega} = \frac{k_j^{-2}}{4(2j+1)} \sum_L A_L^{(j,j')} P_L(\cos\theta), \quad (2.12)$$

where

$$A_L^{(jj')} = (-1)^L (2L+1) \sum_{l_1 l_2 l_1' l_2'} i^{l_1' - l_1 - l_2' + l_2} [(2l_1' + 1)(2l_1 + 1)(2l_2' + 1)(2l_2 + 1)]^{1/2} \\ \times \begin{pmatrix} l_1' & l_2' & L \\ 0 & 0 & 0 \end{pmatrix} \begin{pmatrix} l_1 & l_2 & L \\ 0 & 0 & 0 \end{pmatrix} \sum_{l_t} (-1)^{l_t} (2l_t + 1) \begin{Bmatrix} l_1' & l_2' & L \\ l_2 & l_1 & l_t \end{Bmatrix} T_{j_1' l_1' j_1}^{l_t} T_{j_2' l_2' j_2}^{l_t*}. \quad (2.13)$$

The new T^{l_t} matrix is obtained from the transition matrix T^J by the following relation²²

$$T_{j_1' l_1' j_1}^{l_t} = \sum_J (-1)^J (2J+1) \begin{Bmatrix} j' & j & l_t \\ l & l' & J \end{Bmatrix} T_{j_1' l_1' j_1}^J, \quad (2.14)$$

and the values of l_t are defined by the inequality larger of $(|l - l'|, |j - j'|) \leq l_t$

$$\leq \text{smaller of } (l + l', j + j').$$

The scattering cross section for the transition $j - j'$ is given by

$$\sigma_{j \rightarrow j'} = \frac{\pi k_j^{-2}}{2j+1} A_0^{(jj')} \\ = \frac{\pi k_j^{-2}}{2j+1} \sum_{l_t l_1'} (2l_t + 1) |T_{j_1' l_1' j_1}^{l_t}|^2 \\ = \frac{\pi k_j^{-2}}{2j+1} \sum_{J l_1'} (2J+1) |T_{j_1' l_1' j_1}^J|^2, \quad (2.15)$$

and the momentum-transfer cross section for $j - j'$ transition becomes

$$\sigma_{j \rightarrow j'}^m = \int \frac{d\sigma_{j \rightarrow j'}}{d\Omega} (1 - \cos\theta) d\Omega \\ = \frac{\pi k_j^{-2}}{2j+1} (A_0^{(jj')} - \frac{1}{3} A_1^{(jj')}). \quad (2.16)$$

The coupled radial scattering Eqs. (2.6) are exact and their solution should, in principle, give the correct results for electron-impact rotational transitions in a diatomic molecule. However, slow convergence in the basis channel ($j l$) in the presence of the strong noncentral forces makes the solution of these equations numerically an arduous task.

B. Electron scattering in a molecule-fixed frame of reference

The total wave function for scattering from the Hamiltonian (2.1) in a molecule-fixed frame of reference is expanded as⁸

$$\Psi^{JM\eta}(\vec{r}_1', \dots, \vec{r}_N', \vec{r}'; \vec{R}) = \Phi_0(\vec{r}_1', \dots, \vec{r}_N'; \vec{R}) r^{-1} \\ \times \sum_{l'\lambda'} \left(\frac{2J+1}{8\pi(1+\delta_{0\lambda'})} \right)^{1/2} [Y_{l'\lambda'}(\hat{r}') D_{M\lambda'}^{J*}(\hat{R}) + \eta Y_{l',-\lambda'}(\hat{r}') D_{M,-\lambda'}^{J*}(\hat{R})] f_{l'}^{\lambda'}(r), \quad (2.17)$$

whose parity is $\eta(-1)^J$ with $\eta = (-1)^{J+l} = (-1)^{j'+l'}$. The radial equations, equivalent to Eqs. (2.6), now becomes

$$\left(\frac{d^2}{dr^2} - \frac{l(l+1)}{r^2} + 2(E_T - \epsilon_0) \right) f_l^\lambda(r) \\ = 2(-1)^\lambda (2l+1)^{1/2} \sum_{l'\mu} (2l'+1)^{1/2} \begin{pmatrix} l & l' & \mu \\ 0 & 0 & 0 \end{pmatrix} \begin{pmatrix} l & l' & \mu \\ \lambda & -\lambda & 0 \end{pmatrix} V_\mu(r) f_{l'}^\lambda(r) + 2B \sum_{\lambda' j} \Omega_{\lambda' j}^{(l' j \eta)*} j(j+1) \Omega_{j \lambda}^{(l j \eta)} f_l^{\lambda'}(r). \quad (2.18)$$

In deriving the coupled Eqs. (2.18) we have used the multipole expansion (2.8) and the unitary transformation operator Ω , given by⁸

$$\Omega_{j \lambda}^{(l j \eta)} = (-1)^{-j+l+\lambda} (2j+1)^{1/2} \\ \times \begin{pmatrix} j & l & J \\ 0 & \lambda & -\lambda \end{pmatrix} \frac{1 + \eta(-1)^{J-j-l}}{[2(1+\delta_{0\lambda})]^{1/2}}, \quad (2.19)$$

is such that

$$u_{j l}^{J \eta}(r) = \sum_{\lambda} f_l^\lambda(r) \Omega_{\lambda j}^{(l j \eta)*} \quad (2.20)$$

and

$$f_l^\lambda(r) = \sum_j u_{j l}^{J \eta}(r) \Omega_{j \lambda}^{(l j \eta)}. \quad (2.21)$$

(In these two equations we have introduced a superscript η on functions u and f to denote their parities explicitly.) A transformation from a body to the space frame, or vice versa, is merely a geometrical transformation and does not change the dynamics of the collision problem.

C. Fixed-nuclei approximation and the frame-transformation theory

The body-frame scattering Eq. (2.18) can be further simplified by making an approximation. On comparing the two terms on the right-hand side of this equation, one will notice that owing to the smallness of the rotational constant B ($\approx 7.30 \times 10^{-3}$ eV for the lighter most molecule H_2) there will be a region of the configuration space close to the nuclei where first of these two terms will dominate the whole scattering process. The multipole terms V_μ are usually very strong in the neighborhood of the nuclei for higher val-

ues of μ (see Fig. 1 of I and Ref. 24). The neglect of those terms which contain the rotational constant B should have very little effect on the solutions of the body-frame equations in this inner part of the configuration space.

After dropping H_{rot} in the molecular-core region, the Hamiltonian (2.1) then describes merely the electronic motion of the colliding systems. This essentially means invoking the zeroth-order (fixed-nuclei) approximation in the Born-Oppenheimer separation²⁵ of the electronic and nuclear motions. The body-frame radial scattering Eq. (2.18) takes up the following simple form:

$$\left(\frac{d^2}{dr^2} - \frac{l(l+1)}{r^2} + k^2\right)f_i^\lambda(r) = 2(-1)^\lambda(2l+1)^{1/2} \sum_{l'\mu} (2l'+1)^{1/2} \begin{pmatrix} l & l' & \mu \\ 0 & 0 & 0 \end{pmatrix} \begin{pmatrix} l & l' & \mu \\ \lambda & -\lambda & 0 \end{pmatrix} V_\mu(r) f_i^{\lambda'}(r), \quad (2.22)$$

where $k^2 = 2(E_r - \epsilon_0)$, in the fixed-nuclei approximation.^{1,10,26-28}

These equations are based upon the single-center expansion

$$\phi_\alpha(\vec{r}') = r^{-1} \sum_I \varphi_I^\alpha(r) Y_{Im_\alpha}(\hat{r}') \quad (2.23)$$

of the bound and

$$F^\lambda(\vec{r}') = r^{-1} \sum_I f_I^\lambda(r) Y_{I\lambda}(\hat{r}') \quad (2.24)$$

of the continuum molecular orbitals about the center of mass of the molecule.

A molecule-fixed frame of reference, however, does not necessarily mean a fixed-nuclei approximation unless one neglects the splitting of the rotational levels of the molecule, i.e., the nuclei become infinitely massive. The neglect of the nuclear rotation in the inner region in a body frame have changed the physics of the problem in this region. The inner and outer regions describe the electron-molecule scattering in body- and space-fixed frames of reference, respectively, where two entirely different physical situations prevail. Although a transformation from one frame to the other is still carried out by the energy-independent operator (2.19), it is no longer merely a geometrical transformation as the words frame transformation may imply. Instead, in going from inner (body frame) to the outer region (lab frame) the dynamical approximations describing the collision problem also change.

The essential approximation which one makes in deriving the fixed-nuclei Eq. (2.22) from the body frame Eq. (2.18) is that the effect of the rotational energy terms of the molecule [second term on the right-hand side of Eq. (2.18)] can be neglected from the energy k^2 (in Ry) of the in-

cident electron. Although the correct energy factor in a given channel should be $k^2(J, l)$ [in the lab frame $k^2(J, l) = k_j^2$ from Eq. (2.7)] but in the fixed-nuclei approximation this quantity simply becomes k^2 . The effect of this difference on the electron scattering in any region will be a minimal if the potential energy on the right-hand side of the fixed nuclei Eq. (2.22) is large compared to $k^2 - k^2(J, l)$. If the value of the inner molecular-core radius r_i becomes so big that this condition is not satisfied, then the fixed-nuclei approximation in that region will certainly break down. One shall have to terminate the inner region at smaller values of r_i and introduce the space-frame treatment in the outer region for $r \geq r_i$.

However, under certain circumstances [e.g., when the impact energy of the incident electron is so high that owing to the smallness of B the difference in between k^2 and $k^2(J, l)$ itself becomes negligible and/or the long-range terms of the interaction potential fall off rapidly] it is possible that the integration of the lab frame Eq. (2.6) in the outer region may not make a significant contribution to the scattering. (A situation similar to this was discovered by Henry and Chang¹⁵ and Chang¹⁶ in their study of the simultaneous vibration-rotation excitation in e^- - H_2 scattering.) The phase shift obtained by considering the scattering only in the inner region in a body frame in fixed-nuclei approximation will be accurate enough and a space-frame treatment in the outer region will not be required, i.e., most of the phase accumulation will take place from the solution of the fixed-nuclei equations in the region $0 \leq r \leq r_i$. The adiabatic-nuclei approximation² can now be used to calculate the cross sections for electron-impact vibration-rotation transitions in a diatomic molecule.

The frame-transformation theory of electron-molecule scattering is, therefore, particularly useful when the energy of the incident electron is low and/or the interaction potential consists of sufficiently long-range (e.g., r^{-1} , r^{-2} , etc., type) terms which do not fall off very rapidly.

III. METHOD OF IMPLEMENTATION OF THE FRAME-TRANSFORMATION THEORY

A. Definition and calculation of \underline{R} matrix

In formulating the FT theory of electron-molecule scattering, Chang and Fano⁸ have suggested the transformation of the solutions and derivatives of the body-frame fixed-nuclei Eq. (2.22) at point r_t to the lab frame in going from inner to the outer region. Consequently, one has to perform two separate transformations. Recently, the \underline{R} -matrix theory, developed by Wigner and Eisenbud¹⁴ for nuclear reactions,²⁹ has been used very extensively in electron-atom scattering calculations.³⁰ Here, while considering the scattering only in one (usually laboratory) frame of reference, the interior part ($r \leq r_t$) includes both the local and nonlocal short-range interactions and the outer part ($r \geq r_t$) consists of only the long-range terms of the local potential. This natural division of the whole interaction space in two parts, supplemented merely by a similarity transformation of a matrix from body to lab frame in going from inner to the outer region, makes it very convenient to use the \underline{R} -matrix method for studying electron-molecule scattering in the context of the FT theory.

We adopt the same definition of the \underline{R} matrix as given by Burke and Robb,³⁰ namely,

$$\underline{R}(r_t) = [\underline{\omega}(r) \{ \underline{r} \underline{\omega}'(r) - \underline{b} \underline{\omega}(r) \}^{-1}]_{r=r_t}, \quad (3.1)$$

where $\underline{\omega}(r)$ and $\underline{\omega}'(r)$ are a set of linearly independent solutions of Eq. (2.22) and their derivatives, respectively, and \underline{b} is an arbitrary constant matrix. If \underline{b} is taken to be a null matrix the expression (3.1) can be looked upon as the logarithmic derivative matrix of the solutions at $r=r_t$. A set of linearly independent solutions of (2.22) can be related to another set by a transformation

$$\underline{v}(r) = \underline{A} \underline{\omega}(r), \quad (3.2)$$

where \underline{A} is a nonsingular matrix which is independent of r . After substituting (3.2) into (3.1) we find

$$\underline{R}(r_t) = [\underline{v}(r) \{ \underline{r} \underline{v}'(r) - \underline{b} \underline{v}(r) \}^{-1}]_{r=r_t},$$

i.e., the \underline{R} matrix of Eq. (3.1) is independent of the choice of the set of linearly independent solutions of an equation.

In order to form the sets $\underline{\omega}(r)$ and $\underline{\omega}'(r)$, we integrate the fixed-nuclei Eq. (2.22) in the region

from 0 to r_t with the following boundary conditions

$$\begin{aligned} f_{i\nu}^\lambda &\underset{r \rightarrow 0}{\sim} r^{l+1} \delta_{i\nu}, \\ f_{i\nu}^\lambda(r_t) &= k^{-1/2} [j_l(kr_t) \delta_{i\nu} + \eta_l(kr_t) \mathcal{K}_{i\nu}^\lambda] r_t. \end{aligned} \quad (3.3)$$

Here, $j_l(x)$ and $n_l(x)$ are, respectively, the regular and irregular spherical Bessel functions such that

$$j_l(x) \underset{x \rightarrow \infty}{\sim} (1/x) \sin(x - \frac{1}{2} l\pi)$$

and

$$\eta_l(x) \underset{x \rightarrow \infty}{\sim} (1/x) \cos(x - \frac{1}{2} l\pi).$$

(Note that in the fixed-nuclei approximation all channels will be open and degenerate.) The second subscript on f^λ in Eq. (3.3) stands for the incident channel. The \mathcal{K}^λ matrix calculated from Eq. (3.3) is not the correct \underline{K} matrix as no account has been taken of the long-range terms in the inner region ($0 \leq r \leq r_t$) in the solution of the fixed-nuclei equations. Instead, the calculation of \mathcal{K}^λ is based completely upon the inclusion of the short-range terms of local and nonlocal electron-molecule interaction potential in the scattering Eq. (2.22) in the molecular-core region.³¹

The convergence of the eigenphase sum

$$\delta_{\text{sum}}^\lambda = \text{Tr} [\tan^{-1}(\underline{B} \mathcal{K}^\lambda \underline{B}^{-1})] \quad (3.4)$$

will now completely depend upon the inclusion of the highly anisotropic short-range terms and the two nuclear singularities in the fixed-nuclei Eq. (2.22). In Eq. (3.4), \underline{B} is an orthogonal matrix which diagonalizes the real symmetric \mathcal{K}^λ matrix. The convergence of $\delta_{\text{sum}}^\lambda$ will, in fact, determine whether the single-center expansion (2.24) in l of the continuum molecular orbital and the multipole expansion (2.8) in μ of the molecular charge distribution have converged.

The solution elements $f_{i\nu}^\lambda$, and their derivatives $f_{i\nu}^\lambda$ are now linearly combined

$$\begin{aligned} \omega_{ij}^\lambda(r) &= \sum_{k=1}^{n_e} a_{ik} f_{kj}^\lambda(r), \\ \omega_{ij}^\lambda(r) &= \sum_{k=1}^{n_e} a_{ik} f_{kj}^\lambda(r), \end{aligned} \quad (3.5)$$

(where $i, j = 1, \dots, n_e$, the number of coupled equations), to form a set of linearly independent solutions $\underline{\omega}^\lambda(r)$ and their derivatives $\underline{\omega}^\lambda(r)$. The generic program³² written by us describes in detail the method of solving and matching a set of coupled homogeneous (or inhomogeneous) scattering equations to the asymptotic scattering boundary conditions. This program could be readily adapted to the choice of the boundary conditions given in Eq. (3.3). The matching procedure, needed to calculate \mathcal{K}^λ matrix, also yields³² the coefficients of linear combination a 's used in Eqs. (3.5). These

sets of $\omega^\lambda(r)$ and $\omega^\lambda(r)$ can now be employed for calculating the \underline{R}^λ matrix at point $r=r_t$ in a molecule-fixed frame of reference in fixed-nuclei approximation:

$$\underline{R}^\lambda(r_t) = \{\underline{\omega}^\lambda(r) [\underline{r}\underline{\omega}^\lambda(r) - \underline{b}\underline{\omega}^\lambda(r)]^{-1}\}_{r=r_t}. \quad (3.6)$$

This matrix will obviously be diagonal in λ and have the dimensions equal to the number of l values of the single-center expansion (2.24) that are coupled in Eq. (2.22).

B. Transformation of \underline{R}^λ matrix and calculation of \underline{S}^J matrix

In the outer region ($r_t \leq r \leq \infty$) the space-fixed frame treatment of the scattering process is described by Eq. (2.6). The terms V_μ of the electron-molecule interaction potential now consist of only a first few long-range multipole moments, permanent or induced, of the molecular charge distribution. The coupled radial Eqs. (2.6) are integrated inward from $r = \infty$ to $r = r_t$. The asymptotic forms given in Eqs. (2.9) determine the boundary conditions to be used to start an inward integration from $r = \infty$ in order to generate a family of solutions. If n_0 is the number of open channel basis sets ($jl \equiv p$) out of the total number n_t coupled in Eq. (2.6), a set of n_0 linearly independent solutions and derivatives is obtained from

the following combinations,

$$\begin{aligned} \nu_{pr}^{J\eta} &= \sum_{q=1}^{n_t+n_0} c_{pq} u_{qr}^{J\eta}, \\ \nu_{pr}^{J\eta'} &= \sum_{q=1}^{n_t+n_0} c_{pq} u_{qr}^{J\eta'}, \end{aligned} \quad (3.7)$$

of the elements of solutions of Eq. (2.6) and their derivatives, respectively. Here, we have introduced the superscript $\eta = (-1)^{j+l} = (-1)^{j'+l'}$ specifying the parity $[=(-1)^J]$ of the basis set coupled in Eq. (2.6). In order to determine the coefficients c 's in Eq. (3.7) we form the $\underline{R}^{J\eta}$ matrix at $r=r_t$, i.e.,

$$\underline{R}^{J\eta}(r_t) = \{\underline{\nu}^{J\eta} [\underline{r}\underline{\nu}^{J\eta}(r) - \underline{b}\underline{\nu}^{J\eta}(r)]^{-1}\}_{r=r_t}, \quad (3.8)$$

where constant matrix \underline{b} is the same as used in Eq. (3.6).

This matrix should be equal to the $\underline{\mathcal{R}}^{J\eta}(r_t)$ matrix obtained by transforming to the space frame the $\underline{R}^\lambda(r_t)$ matrix of Eq. (3.6) which has been calculated in the body frame of reference in fixed-nuclei approximation. Therefore

$$\underline{\nu}^{J\eta}(r_t) = \underline{\mathcal{R}}^{J\eta}(r_t) [\underline{r}\underline{\nu}^{J\eta}(r) - \underline{b}\underline{\nu}^{J\eta}(r)]. \quad (3.9)$$

The elements of $\underline{\mathcal{R}}^{J\eta}(r_t)$ matrix are given by a similarity transformation of the $\underline{R}^\lambda(r_t)$ matrix carried out by the orthogonal transformation operator Ω of Eq. (2.19). Therefore,

$$\begin{aligned} \mathcal{R}_{j'l',j'l'}^{J\eta} &= \sum_{\lambda \geq 0}^{\lambda_{\min}} \Omega_{\lambda_j}^{(jJ\eta)T} R_{ll'}^\lambda \Omega_{\lambda_{j'}}^{(j'J\eta)} \\ &= 2[(2j+1)(2j'+1)]^{1/2} \sum_{\lambda \geq 0}^{\lambda_{\min}} \begin{pmatrix} j & l & J \\ 0 & \lambda & -\lambda \end{pmatrix} \frac{R_{ll'}^\lambda}{1+\delta_{0\lambda}} \begin{pmatrix} j' & l' & J \\ 0 & \lambda & -\lambda \end{pmatrix}, \end{aligned} \quad (3.10)$$

where λ_{\min} is the smaller of (l, l', J) . Because for linear molecules $\underline{R}^{-\lambda} = \underline{R}^\lambda$ [see Eq. (2.22)], this transformation can also be written as³³

$$\begin{aligned} \mathcal{R}_{j'l',j'l'}^{J\eta} &= [(2j+1)(2j'+1)]^{1/2} \\ &\times \sum_{\lambda = -\lambda_{\min}}^{\lambda_{\min}} \begin{pmatrix} j & l & J \\ 0 & \lambda & -\lambda \end{pmatrix} R_{ll'}^\lambda \begin{pmatrix} j' & l' & J \\ 0 & \lambda & -\lambda \end{pmatrix}. \end{aligned} \quad (3.11)$$

The matrix of Eq. (3.11) is now substituted on the right-hand side of Eq. (3.9). Burke *et al.*³⁴ have discussed in detail the solution of the matching Eq. (3.9) in their formulation of the \underline{R} -matrix theory of electron-atom scattering. They have also derived the appropriate expressions relating the \underline{K} matrix to the coefficients of linear expansion used in Eqs. (3.7). Once $\underline{K}^{J\eta}$ matrix is known one can always compute the $\underline{S}^{J\eta}$ matrices from Eqs. (2.10) and (2.11), respectively, in order to calcu-

late the differential and integrated cross sections³⁵ for electron-impact rotational transitions in a diatomic molecule.

The whole procedure of employing the FT theory to study electron-molecule scattering can, therefore, be divided into five following steps: (i) study the convergence of the fixed-nuclei Eq. (2.22) in the inner region ($0 \leq r \leq r_t$) in l and μ , (ii) compute body-frame \underline{R}^λ matrix at $r=r_t$ for all values of $\lambda \leq \lambda_{\min}$, (iii) transform the \underline{R}^λ matrix to $\underline{\mathcal{R}}^{J\eta}$ matrix, (iv) solve the space-frame Eqs. (2.6) in the outer region ($r \geq r_t$) by integrating inward from $r = \infty$ to $r = r_t$ and match the solutions and derivatives with $\underline{\mathcal{R}}^{J\eta}$ matrix for calculating the $\underline{\mathcal{K}}^{J\eta}$ -matrix, and (v) calculate the $\underline{S}^{J\eta}$ matrix from Eq. (2.10) and then the cross sections for different rotational transitions.

In addition to this, one will also have to study the dependence of the final cross sections on the choice of the boundary point r_t where the inner

and the outer region are separated from each other. This will involve trying a number of different values for r_t and then deciding upon that particular value where the results are fairly "stabilized." This point has been further discussed at length in Sec. IV B 3.

The last three steps, out of the above five required for the successful implementation of the FT theory, have to be carried out both for even and odd parities, i.e., for $\eta = +1$ and -1 values, for the same value of J . However, it may also be necessary to study the convergence of the lab-frame Eqs. (2.6) in the number of coupled channels (jl) in the outer region ($r \geq r_t$). In that case, steps (iii) to (v) will have to be repeated each time by increasing the number of coupled rotational states in the outer region for each J and η values.

IV. NUMERICAL CALCULATIONS

A. Test study: application to a model calculation

The practical application of the FT theory is a multistep process which becomes an arduous task. We therefore thought it to be extremely useful to apply this theory first to some model calculation of e^- -CO scattering before using it in more fundamental and complex situations. This test study will also make the physics of the problem more transparent and at the same time provide a good check on our whole numerical procedure.

Crawford and Dalgarno¹⁸ have studied the scattering of thermal-energy electrons from carbon monoxide using the close-coupling (c.c.) formulation of Arthurs and Dalgarno.³ (The method has accordingly been called rotational close coupling.) Their whole calculation has been done in the space-fixed frame by solving the Eq. (2.6). They employ a semiempirical potential which is a combination of the dipole, quadrupole, and polarization potentials of carbon monoxide. This potential, in the notation of Eq. (2.8), can be written as

$$V_0(r) = -\frac{\alpha_0}{2(r^2 + r_0^2)^2},$$

$$V_1(r) = \begin{cases} 0 & r \leq r_d, \\ \frac{D}{r^2} \frac{(r - r_d)^2}{b_d^2 + (r - r_d)^2} & r \geq r_d, \end{cases} \quad (4.1)$$

and

$$V_2(r) = V_2^{(a)}(r) + V_2^{(b)}(r),$$

where

$$V_2^{(a)}(r) = \begin{cases} 0 & r \leq r_a, \\ \frac{Q}{r^3} \frac{(r - r_a)^2}{b_a^2 + (r - r_a)^2} & r \geq r_a, \end{cases}$$

and

$$V_2^{(b)}(r) = \begin{cases} 0 & r \leq r_p, \\ -\frac{\alpha_2}{2(r^2 + r_0^2)^2} \frac{(r - r_p)^2}{b_p^2 + (r - r_p)^2} & r \geq r_p. \end{cases}$$

In this expansion (all quantities are in atomic units, unless specified otherwise)

$$D = 0.044, \quad Q = -1.859, \quad \alpha_0 = 13.342, \quad \alpha_2 = 2.396 \quad (4.2)$$

are, respectively, the dipole moment, quadrupole moment, spherical, and the nonspherical components of the polarizability of CO molecule. r_0 , r_a , b_d , r_a , b_a , r_p , and b_p are seven disposable parameters. Crawford and Dalgarno¹⁸ arbitrarily fixed the last six parameters at the outset, but they varied r_0 so that the potential (4.1) while used in Eq. (2.6) would give the experimental value⁹ of the momentum transfer cross section at 0.03 eV. This potential could then reproduce the momentum transfer cross section measured by Hake and Phelps⁹ in the energy range 0.005–0.10 eV. The asymptotic form of potential (4.1) is

$$V_0(r) \sim -\alpha_0/2r^4,$$

$$V_1(r) \sim D/r^2, \quad (4.3)$$

and

$$V_2(r) \sim Q/r^3 - \alpha_2/2r^4.$$

Before using the FT theory, we first used this potential to study the electron scattering in the fixed-nuclei approximation in the whole region of configuration space. We employed the program of Ref. 32 to solve Eq. (2.22) in the region $0 \leq r \leq \infty$. The solution of these equations will now give us the exact K^λ matrix of the body frame in fixed-nuclei approximation. This matrix was then used to compute the eigenphase sum defined in Eq. (3.4) for studying the convergence of the single-center expansion (2.24) in l for ${}^2\Sigma(\lambda=0)$, ${}^2\Pi(\lambda=1)$, and ${}^2\Delta(\lambda=2)$ states of the ($e^- + \text{CO}$) system. We found that 8 or 9 values of l were sufficient to achieve satisfactory convergence of the single-center expansion when the model potential of Eq. (4.1) was used. The converged eigenphase sums for these three cases are shown in Fig. 1. There is known to be a shape resonance³⁶ at about 1.75 eV for electron scattering from CO in ${}^2\Pi$ state. We notice from Fig. 1 that the eigenphase sums calculated using the Crawford and Dalgarno potential,¹⁸ given in Eq. (4.1), does not reproduce this resonance. However, there is a resonance behavior shown by the ${}^2\Sigma$ state eigenphase sum at about 1.40 eV. Similarly the ${}^2\Pi$ eigenphase sum too shows a very broad resonance at a higher energy.

In order to employ the FT theory the potential

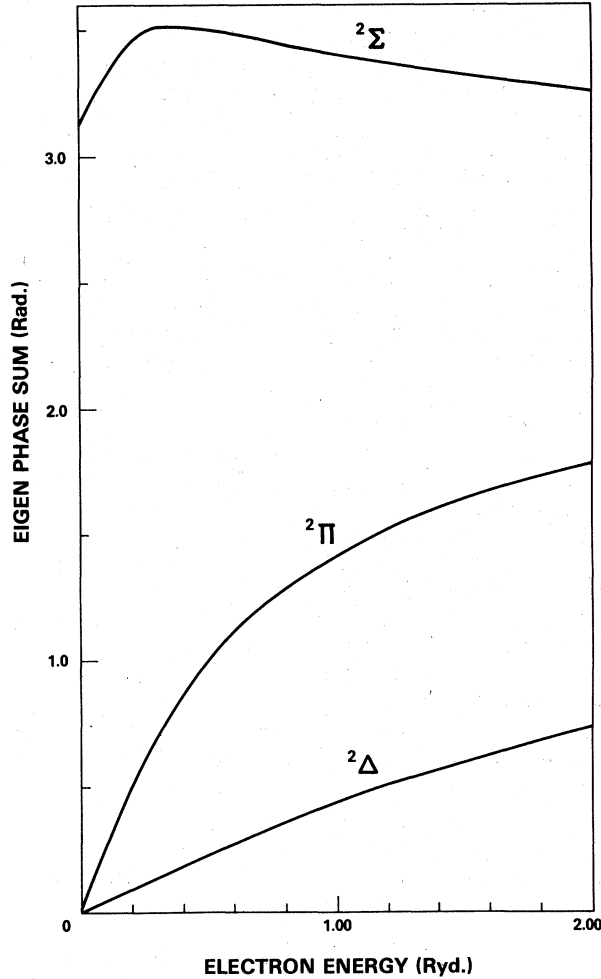


FIG. 1. Eigenphase sum calculated in the fixed-nuclei approximation from the model potential (4.1) of Crawford and Dalgarno (Ref. 18).

(4.1) should be used in the inner region ($0 \leq r \leq r_t$) in the fixed-nuclei approximation. If point r_t is far enough from the center of mass of the molecule, then one is always justified in using the asymptotic form (4.3) of this potential in the lab-frame treatment in the outer region. However, as the potential (4.1) is in a very simple form, we have used the exact potential even in the region for $r \geq r_t$. In order to calculate the cross sections for different rotational transitions from FT theory we have carried out the five-step process mentioned at the end of Sec. III.

A sampling of our partial cross sections $\sigma_{j \rightarrow j'}$, for transitions (0-0), (0-1), (1-1), and (2-2) is shown in Table I for the incident electron energy of 0.05 eV. In the fourth column of this table the exact rotational c.c. results, which we have calculated and agree very well with those of Ref. 18, are also given. In the last five columns, the cross sections calculated from the FT theory for five different values of r_t are tabulated. [The value $b = 1$ was used in Eqs. (3.6) and (3.9) in the definition of R matrix. The partial cross sections calculated for other incident energies had a behavior as a function of r_t similar to those of Table I.]

The very first thing which one should expect from these results is that smaller the value of r_t , the better should be the agreement between the rotational c.c. and FT results. This is due to the fact that the potential used in two regions of the FT theory is exactly the same and it is only the rotational level spacing which has been neglected in the inner region in fixed-nuclei approximation. A decrease in the size of this region will, therefore, mean that the lab-frame rotational c.c. treatment is being introduced closer to the origin. Our results of Table I confirm this general con-

TABLE I. Comparison of $\sigma_{j \rightarrow j'}^j$ (\AA^2) calculated from the frame-transformation theory with the close-coupling results obtained using Crawford and Dalgarno (Ref. 18) potential.

| Energy (eV) | $j \rightarrow j'$ | J | Exact ^a | Frame transformation ($b = 1.0$) ^b , r_t ^{b,c} | | | | |
|----------------|--------------------|-----|--------------------|--|-------|-------|-------|--------|
| | | | | 4.466 | 6.090 | 7.714 | 9.338 | 10.150 |
| 0.05 | 0 → 0 | 0 | 2.251 | 2.243 | 2.243 | 2.243 | 2.242 | 2.242 |
| | | 1 | 0.328 | 0.328 | 0.328 | 0.328 | 0.328 | 0.328 |
| | | 2 | 0.009 | 0.009 | 0.009 | 0.009 | 0.009 | 0.009 |
| | 0 → 1 | 0 | 0.532 | 0.532 | 0.532 | 0.532 | 0.533 | 0.533 |
| | | 1 | 0.874 | 0.874 | 0.874 | 0.874 | 0.874 | 0.874 |
| | | 2 | 0.519 | 0.519 | 0.519 | 0.519 | 0.519 | 0.519 |
| | 1 → 1 | 0 | 0.052 | 0.051 | 0.051 | 0.051 | 0.051 | 0.051 |
| | | 1 | 2.466 | 2.430 | 2.388 | 2.349 | 2.311 | 2.292 |
| | | 2 | 0.111 | 0.114 | 0.115 | 0.116 | 0.117 | 0.117 |
| | 2 → 2 | 0 | 0.003 | 0.003 | 0.003 | 0.003 | 0.003 | 0.003 |
| | | 1 | 0.004 | 0.004 | 0.003 | 0.003 | 0.003 | 0.003 |
| | | 2 | 2.482 | 2.445 | 2.397 | 0.338 | 2.265 | 2.223 |

^aRotational close coupling.

^bSee Eq. (3.6).

^cIn atomic units.

clusion.

We also notice from the entries of this table that the partial cross sections which vary most with the values of r_t are those in which ($l=0, l'=0$) partial wave coupling is present, namely $\sigma^J(j=J \rightarrow j'=J)$. On the other hand, the $\sigma^0(0 \rightarrow 0)$ cross section is almost invariant with the values of r_t considered in this table and at the same time is in good agreement with the exact rotational c.c. results. The major contribution to the ($0 \rightarrow 0$) transition with $J=0$ will basically come from V_0 term of potential (4.1). The form of this term used by Crawford and Dalgarno¹⁸ is such that it has already assumed its asymptotic form much before the space-frame treatment is introduced at $r_t = 4.466$ a.u. [see Eqs. (4.1) and (4.2), $r_0 = 1.310$ a.u. from Ref. 18] and therefore falls off as r^{-4} . As a result the V_0 term has become so small in the outer region that most of the phase accumulation occurs from the solution of the fixed-nuclei equations in the inner region and a lab-frame treatment in the outer region does not make any significant contribution to the scattering. The cross sections for other values of j, j' , and J are almost constant for all values of r_t and they agree very well with those calculated from rotational c.c. method. This kind of behavior of the results calculated from FT theory will, however, very much depend upon the nature of the short-range terms, which are not very strong in the present case.

It should be mentioned at this stage that such

$$\left(\frac{d^2}{dr^2} - \frac{l(l+1)}{r^2} + k^2\right) f_l^\lambda(r) = 2(-1)^\lambda (2l+1)^{1/2} \sum_{\mu'} (2l'+1)^{1/2} \begin{pmatrix} l & l' & \mu \\ 0 & 0 & 0 \end{pmatrix} \begin{pmatrix} l & l' & \mu \\ \lambda & -\lambda & 0 \end{pmatrix} V_\mu(r) f_{l'}^\lambda(r) + \sum_{\alpha=1}^{n_b} \xi_\alpha \varphi_i^\alpha(r). \quad (4.4)$$

Here, $\varphi_i^\alpha(r)$ are the radial coefficients in the single-center expansion (2.23) of the molecular core orbitals $\phi_\alpha(\vec{r}')$ which have the same symmetry as the continuum orbital $F^\lambda(\vec{r}')$ in Eq. (2.24). ξ_α are the Lagrange multipliers determined by the requirement that

$$\langle \phi^\alpha | F^\lambda \rangle = 0$$

for $\alpha = 1, \dots, n_b$, the number of such bound orbitals of a particular symmetry.

As discussed in I, the program of Faisal and Tench³⁷ was employed to convert the two-center ground-electronic-state wave-function of CO, given by McLean and Yoshimine,³⁸ into a one-center expansion about the center of mass of the molecule. These single-center expansions of the molecular orbitals were then used to calculate the multipole expansion (2.8) of the molecular charge distribution.

{We will like to point out to the reader that there

good agreement between the rotational c.c. and FT results is subject to the accuracy to which the fixed-nuclei Eqs. (2.22) are solved in the inner region in order to calculate the R^λ matrix at $r=r_t$. The accuracy of the solutions in the present case simply means that the sufficient values of l are coupled in Eq. (2.22) for the single-center expansion (2.24) of the continuum orbital to converge for each value of λ . However, such a satisfactory solution of the inner-region equation in a body frame of reference in fixed-nuclei approximation is a prerequisite for a successful application of the FT theory for studying the electron-molecule scattering.

B. Application to the single-center pseudopotential method

1. Adaptation of the pseudopotential method to the frame-transformation theory

The pseudopotential method, originally introduced in our $e^- - N_2$ study,¹⁰ has been found to work very well even for electron scattering from CO in the fixed-nuclei approximation. In this method, the exchange effects between the incident and the molecular electrons are simulated by orthogonalizing the continuum scattering orbital to the bound molecular orbitals of the same symmetry. The body-frame fixed-nuclei Eq. (2.22) are now replaced by the following coupled inhomogeneous equations:

is an error in Eq. (17) of Ref. 21 where the electron-nuclei contribution [terms enclosed in the parenthesis on the right-hand side of Eq. (2.4)] to the static potential has been expanded into the Legendre polynomials about the center of mass of the molecule. As the program of Faisal and Tench³⁷ has used this expression to compute the multipole expansion of the molecular charge distribution, the corresponding correction should, therefore, also be made in this program. This error and the correct form of the expression are given in I.]

The highly anisotropic short-range terms, nuclear singularities, and the exchange effects are properly represented in Eq. (4.4) by achieving satisfactory convergences in the expansions (2.8), (2.23), and (2.24) simultaneously. We have shown in I that these three expansions converge very well even for low-symmetry molecules like CO.

In order to have a resonance in the ${}^2\Pi$ eigenphase

sum calculated from (4.4) at about 1.75 eV, the static potential in I was augmented by a polarization potential of the form

$$V_{\text{pol}}(\vec{r}) = -\frac{1}{2r^4} [\alpha_0 + \alpha_2 P_2(\hat{r} \cdot \hat{R})] \left\{ 1 - \exp \left[-\left(\frac{r}{r_0} \right)^6 \right] \right\}, \quad (4.5)$$

where

$$\alpha_0 = 13.342, \quad \alpha_2 = 2.396. \quad (4.6)$$

The adjustable parameter $r_0 = 1.605$ a.u. was found to give a resonance in ${}^2\Pi$ state at $E_r = 1.753$ eV. The calculated values of the width (Γ_r) and background phase shift (δ_r) for this resonance are, respectively, 0.278 eV and -0.082 rad.

In the context of FT theory, we solve Eqs. (4.4), together with the polarization potential (4.5), in the molecular-core region ($0 \leq r \leq r_t$). The method of solving the inhomogeneous equations together with the requirements of orthogonality has been discussed in detail in our previous paper of Ref. 32. This program could be easily adapted to calculate the fixed-nuclei R^λ matrix defined in Eq. (3.6). In the outer region ($r \geq r_t$), on the other hand, we assume that $\varphi_i^{\lambda}(r) \approx 0$ and both the static and the polarization potentials, Eqs. (2.8) and (4.5), respectively, have taken up their asymptotic forms. Therefore, for the space frame Eq. (2.6) in the outer region the potential will be given by

$$V_0(r) = -\frac{\alpha_0}{2r^4}, \quad V_1 = \frac{D}{r^2}, \quad (4.7)$$

$$V_2(r) = \frac{Q}{r^3} - \frac{\alpha_2}{2r^4}, \quad V_3(r) = \frac{O}{r^4},$$

where O is that octopole moment of the CO molecule. The values of α_0 and α_2 are given in Eq. (4.6). But

$$D = -0.105, \quad Q = -1.547,$$

and

$$O = 4.380 \quad (4.8)$$

were obtained from the multipole expansion (2.8) of the CO static potential whose calculation has been described elsewhere.¹

2. Selection of the inner-molecular-core radius r_t

The partial cross sections $\sigma_{j \rightarrow j'}$, obtained by using the single-center pseudopotential in context of the FT theory are given in Table II for six different values of r_t . According to the test study of Sec. IV A, we find that the $\sigma_{j \rightarrow j'}$, for $(j, j' = J)$ cross section varies most with r_t . This is associated with the fact that in this case the s wave is coupled

with both initial and final rotational states.

We have said above, while discussing the adaptation of the pseudopotential to FT theory, that in going from inner to the outer region we completely neglect the short-range parts of the local and non-local electron-molecule interactions. A selection of a smaller value of r_t will, therefore, mean that more of these potential terms are being neglected in performing a frame transformation even though they have not become small enough. On the other hand, performing the transformation at a large distance from the center of mass of the molecule corresponds to the fact that although the potential, which is still non-negligible due to the long-range terms, has become comparable to the rotational level spacings but the latter has not been introduced yet into the scattering equations. The size of the inner-molecular-core region, where the fixed-nuclei approximation is being used, has now become so big that the difference in between $[k^2 - k^2(J, l)]$ is no longer smaller than the potential energy terms and therefore the nuclear rotation can no longer be neglected from the scattering equations. In Table II, there corresponds a region between $r_t = 10.150$ a.u. to $r_t = 13.398$ a.u. where the partial cross sections for all transitions seem to have "stabilized."

Chang and Fano⁸ do not give any rigorous criterion for the selection of the boundary point r_t which divides the interaction region into two parts where two physically different treatments of the scattering process are to be carried out. All their statements concerning the choice of this point are qualitative. We do not see any quantitative way for defining the range of the inner-molecular-core region other than carrying out the FT treatment at a number of different values of r_t and then selecting that value where the various cross sections have become fairly "stationary." From our test study, discussed in the preceding subsection, one will conclude that if the scattering equations in the inner region in fixed-nuclei approximation are solved accurately enough then the final cross sections for electron-impact rotational transitions in a molecule will be very close to the exact values provided a transformation from molecule to the space frame is performed at a point where the results are "stabilized."

In the following calculations we have therefore used $r_t = 11.774$ a.u. for the inner-molecular-core radius. Note that this value of the core radius is almost six times of the equilibrium internuclear separation ($= 2.132$ a.u.) in the ground electronic state of carbon monoxide.

The existence of the boundary point r_t is the central aspect of the FT theory. Selection of two different limiting values for r_t will reduce the FT

TABLE II. $\sigma_{j \rightarrow j'}^f$ (\AA^2) calculated from the frame-transformation using the pseudopotential.

| Energy (eV) | $j \rightarrow j'$ | J | Frame transformation ($b=1.0$), ^a r_t ^b | | | | | |
|----------------|--------------------|-----|---|--------|--------|--------|--------|--------|
| | | | 6.902 | 8.526 | 10.150 | 11.774 | 13.398 | 15.022 |
| 0.005 | 0 \rightarrow 0 | 0 | 0.990 | 1.341 | 1.452 | 1.485 | 1.495 | 1.497 |
| | | 1 | 0.142 | 0.138 | 0.137 | 0.137 | 0.137 | 0.137 |
| | | 2 | 0.024 | 0.023 | 0.023 | 0.023 | 0.023 | 0.023 |
| | 0 \rightarrow 1 | 0 | 23.319 | 22.867 | 22.820 | 22.812 | 22.810 | 22.810 |
| | | 1 | 54.900 | 53.848 | 53.744 | 53.727 | 53.723 | 53.721 |
| | | 2 | 32.352 | 31.787 | 31.745 | 31.742 | 31.742 | 31.742 |
| | 1 \rightarrow 1 | 0 | 0.189 | 0.188 | 0.187 | 0.187 | 0.187 | 0.187 |
| | | 1 | 0.987 | 1.343 | 1.448 | 1.457 | 1.435 | 1.397 |
| | | 2 | 0.172 | 0.166 | 0.166 | 0.165 | 0.165 | 0.165 |
| | 2 \rightarrow 2 | 0 | 0.008 | 0.008 | 0.008 | 0.008 | 0.008 | 0.008 |
| | | 1 | 0.122 | 0.121 | 0.120 | 0.120 | 0.120 | 0.120 |
| | | 2 | 1.816 | 2.345 | 2.489 | 2.463 | 2.352 | 2.185 |
| 0.05 | 0 \rightarrow 0 | 0 | 5.614 | 6.305 | 6.519 | 6.582 | 6.600 | 6.605 |
| | | 1 | 0.211 | 0.208 | 0.207 | 0.207 | 0.207 | 0.207 |
| | | 2 | 0.011 | 0.011 | 0.011 | 0.011 | 0.011 | 0.011 |
| | 0 \rightarrow 1 | 0 | 2.397 | 2.307 | 2.286 | 2.280 | 2.278 | 2.278 |
| | | 1 | 4.340 | 4.206 | 4.179 | 4.171 | 4.167 | 4.166 |
| | | 2 | 3.008 | 2.955 | 2.951 | 2.951 | 2.951 | 2.951 |
| | 1 \rightarrow 1 | 0 | 0.054 | 0.054 | 0.054 | 0.054 | 0.054 | 0.054 |
| | | 1 | 5.551 | 6.284 | 6.487 | 6.513 | 6.474 | 6.406 |
| | | 2 | 0.074 | 0.073 | 0.073 | 0.074 | 0.075 | 0.076 |
| | 2 \rightarrow 2 | 0 | 0.003 | 0.003 | 0.003 | 0.003 | 0.003 | 0.003 |
| | | 1 | 0.011 | 0.011 | 0.011 | 0.011 | 0.011 | 0.010 |
| | | 2 | 5.656 | 6.491 | 6.719 | 6.692 | 6.540 | 6.311 |
| 0.10 | 0 \rightarrow 0 | 0 | 7.588 | 8.324 | 8.550 | 8.615 | 8.634 | 8.638 |
| | | 1 | 0.327 | 0.320 | 0.318 | 0.317 | 0.317 | 0.317 |
| | | 2 | 0.022 | 0.022 | 0.022 | 0.022 | 0.022 | 0.022 |
| | 0 \rightarrow 1 | 0 | 0.919 | 0.862 | 0.846 | 0.840 | 0.839 | 0.839 |
| | | 1 | 1.843 | 1.764 | 1.744 | 1.738 | 1.735 | 1.734 |
| | | 2 | 1.502 | 1.475 | 1.473 | 1.473 | 1.474 | 1.474 |
| | 1 \rightarrow 1 | 0 | 0.033 | 0.034 | 0.034 | 0.034 | 0.034 | 0.033 |
| | | 1 | 7.507 | 8.292 | 8.508 | 8.537 | 8.500 | 8.438 |
| | | 2 | 0.120 | 0.118 | 0.119 | 0.121 | 0.124 | 0.129 |
| | 2 \rightarrow 2 | 0 | 0.002 | 0.002 | 0.002 | 0.002 | 0.002 | 0.002 |
| | | 1 | 0.002 | 0.002 | 0.002 | 0.002 | 0.002 | 0.002 |
| | | 2 | 7.386 | 8.278 | 8.526 | 8.511 | 8.374 | 8.167 |

^aSee Eq. (3.6).^bIn atomic units.

theory to two well known formulations of the electron-molecule scattering—for $r_t = 0$ it will reduce to the rotational c.c. theory of Arthurs and Dalgarno³ and for $r_t = \infty$ become equivalent¹⁷ to the adiabatic-nuclei theory.² The existence of a value of r_t in between these two limits, therefore, becomes a vital point for the applicability of the FT theory. But at the same time the absence of a rigorous criterion for deciding upon the inner molecular radius r_t makes this theory less fundamental than, say, the rotational c.c. formulation of Arthurs and Dalgarno.³ The stabilization requirement used by us in choosing a value for r_t when performing a transformation from molecule- to a space-fixed frame of reference constitutes probably the best criterion under the existing circumstances. Although this condition too lacks an ele-

ment of rigorousness, it is nevertheless significant that one can obtain more accurate and reliable results with it.

An alternative way for finding a value for the core radius will be to try to fit the cross sections computed from the FT theory to the experimental measurements. Although this fitting procedure will be free from all sorts of uncertainties which may be embedded in the stabilization criterion but at the same time it will make the whole theory more phenomenological.

However, under certain circumstances—e.g., when the information about the molecular-core region can be extracted from the experimental data—it is possible to bypass the difficulties associated with the selection of a proper value for r_t . Fano,³⁹ while analyzing the high-resolution photo-

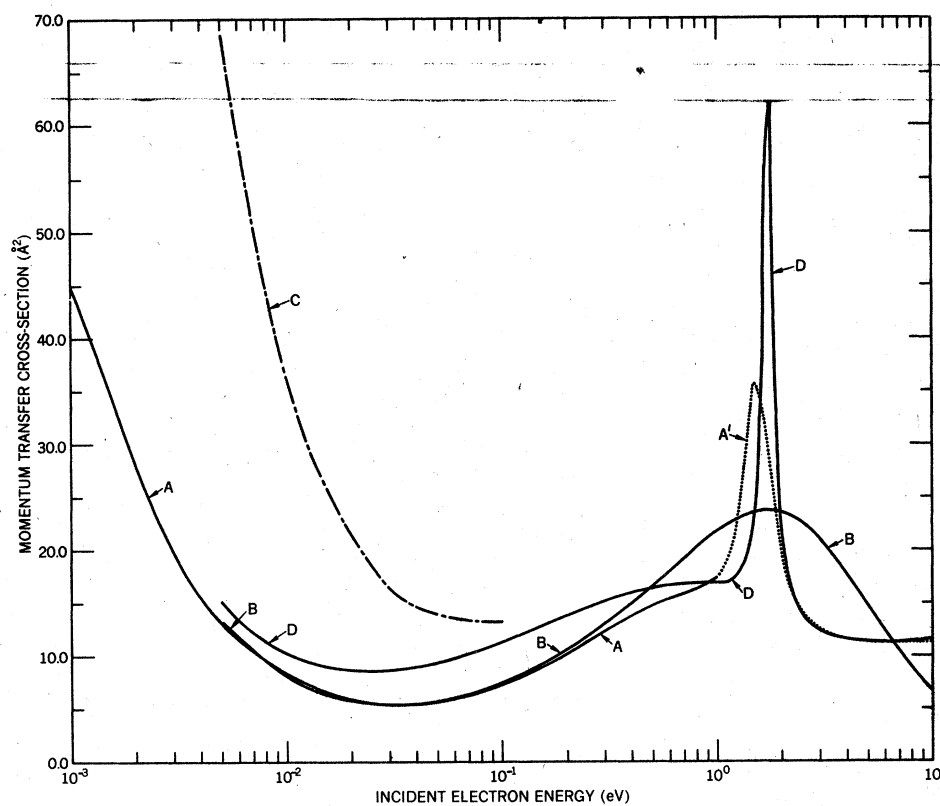


FIG. 2. Comparison of the momentum-transfer cross section $\sigma^m(0)$ vs incident electron energy obtained from different methods. A are the results of Hake and Phelps (Ref. 9) inferred from the swarm experiments with the dotted curve A' obtained so that it extrapolates smoothly to the derived results of A below 1.00 eV. B is calculated by solving the rotational close-coupling Eqs. (2.6) with the potential (4.1) of Crawford and Dalgarno (Ref. 18). C and D represent the results obtained by using the single-center pseudopotential method with the frame-transformation theory: the broken curve C corresponds to the original dipole term in the static potential; the continuous curve D shows the final results of the renormalized dipole term in the static potential.

absorption spectrum of H_2 , and Atabek *et al.*,⁴⁰ calculating the spectrum of Π_u^- Rydberg levels of H_2 , using the FT theory, have obtained the information about the core region of hydrogen molecule from the multichannel quantum defect methods developed by Seaton.⁴¹

We have now specified all the necessary quantities for the inner and outer region required to apply the FT theory to study the e^- -CO scattering using the pseudopotential method. The thermal-energy momentum-transfer cross section, $\sigma^m(0)$ [Eq. (2.16)], calculated from this method is shown by (dash-dot) curve C in Fig. 2. The ratio of the theoretical results to that experimentally measured (curve A) drops from a factor of five at 0.005 eV to about a factor of two at 0.1 eV. We have given in I an analytic proof to show that, unlike the total scattering cross section, the momentum-transfer cross section, averaged over all molecular orientations, is finite even for electron scattering from a polar molecule in a body-fixed frame of reference in the fixed-nuclei approximation. Therefore at higher energies the momentum-transfer cross section calculated from the pseudopotential using the FT theory should be the same as given in Fig. 8 of I where it was computed in the fixed-nuclei approximation. One will also notice that our cal-

culated results in I does reproduce the 1.75-eV ${}^2\Pi$ resonance.

3. Renormalization of the dipole term in the static potential of CO molecule

The electron-polar-molecule scattering at sufficiently low energies is very much dominated by the long-range electron-dipole interaction.⁴² The values of the dipole, quadrupole, and octopole moments which we have used in our pseudopotential method are given in Eq. (4.8). (These values are in good agreement with those computed in Ref. 38; $D = -0.1007$, $Q = -1.634$.) McLean and Yoshimine³⁸ have employed an extended-basis set in the expansion of their two-center wave function with 17 STAO centered on each of the carbon and oxygen nuclei. This sophisticated wave function reproduces the correct ground-electronic-state energy for the equilibrium internuclear separation of CO, the theoretical quadrupole moment (-1.547 a.u.) is about 83% of the experimental value (-1.859 a.u.) but the magnitude of the dipole moment (0.105 a.u.) obtained from this wave function is about 2.4 times higher than the experimentally measured value (0.044 a.u.) [cf. Eqs. (4.2) and (4.8)]. (Also, the theoretically calculated dipole

moment has a sign opposite to that of the experimentally measured. This discrepancy in sign is related to the polarity of CO molecule and the direction of the internuclear axis which have been discussed in Ref. 38.) It will make a difference in the thermal energy electron-scattering cross sections for $j \rightarrow j \pm 1$ transitions approximately by a factor of $(2.4)^2$ [see Eqs. (A12) and (A13) in the Appendix.]

We therefore thought that the easiest way to rectify the shortcoming of the present wave function, without affecting its other properties, which are in conformity with the experiments, would be to scale down the dipole term in the multipole expansion (2.8) by a factor of

$$\zeta_d = |D_{\text{theory}}| / D_{\text{exp}} = 2.386. \quad (4.9)$$

This renormalization of only the dipole term will ensure its continuity over the whole range of the interaction space while other multipole terms will remain unchanged. The multipole expansion (2.8) of the static potential will now be replaced by

$$V(\vec{r}, \vec{R}) = \sum_{\mu} \frac{V_{\mu}(r)}{[1 + (\zeta_d - 1)\delta_{\mu 1}]} P_{\mu}(\hat{r} \cdot \hat{R}) \quad (4.10)$$

in the fixed-nuclei Eq. (4.4). This rescaling of the V_1 term should not alter significantly the short-range nature of the charge distribution of carbon monoxide computed from the wave function of McLean and Yoshimine.³⁸

To consider the constant ζ_d as a parameter in the usual sense of the word perhaps will not constitute a correct description of the present situation. The value $\zeta_d = 2.386$ has not been arrived at by fitting our results to any of the quantities which we intend to calculate finally. The circumstances, on the other hand, have forced us to rescale the dipole term of the static potential by ζ_d in order to correct, rather in a phenomenological way, the deficiency of the ground-electronic-state wave function of CO molecule whose calculation in itself is a major field of research in the domain of quantum chemistry and not the aim of the present study.

Although renormalization of only the dipole term will not affect the convergence properties of the single-center expansions (2.23) and (2.24) and also of the multipole expansion (4.10) in the fixed-nuclei Eq. (4.4), which we have discussed in detail in I; but it will certainly require a new value for the parameter r_0 used in the polarization potential (4.5) in order to have a resonance in the ${}^2\Pi$ state eigenphase sum at about 1.75 eV. The procedure described in I was repeated again but this time only for the ${}^2\Pi$ state. The new value of this parameter obtained was $r_0 = 1.541$ a.u. which is not very much different than the old one (1.605). The new eigenphase sum have been plotted in Fig. 3 and the val-

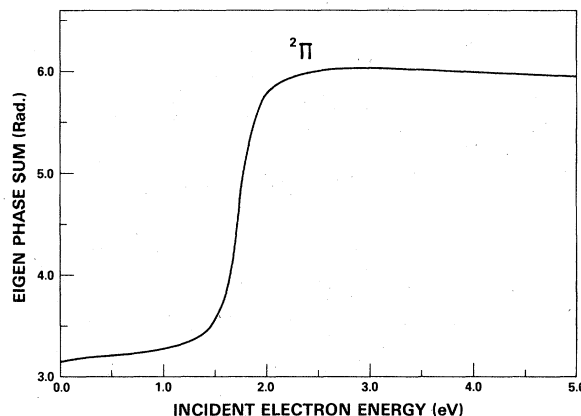


FIG. 3. Eigenphase sum calculated in the fixed-nuclei approximation using the single-center pseudopotential method. The dipole term in the static potential has been renormalized by ζ_d [Eq. (4.10)] and $r_0 = 1.541$ a.u. in the polarization potential (4.5).

ues of the resonance parameters in the present case are $E_r = 1.740$ eV, $\Gamma_r = 0.242$ eV, and $\delta_0 = -0.067$ rad. One will notice that the effect of renormalization of the dipole term on the values of δ_0 and Γ_r is very insignificant indeed. Also this rescaling will not affect the value of the molecular-core radius $r_t = 11.774$ a.u. defining the inner region of the FT theory. Moreover, the new values of the multipole moments required to specify the potential (4.7) in the outer region in a lab frame are now given by

$$\begin{aligned} D &= -0.044, & Q &= -1.547, & O &= 4.380, \\ \alpha_0 &= 13.342, & \alpha_2 &= 2.396, \end{aligned} \quad (4.11)$$

which differ from the old constants, given in Eq. (4.8), in the magnitude of the dipole moment only.

4. Convergence in the outer region

The last thing to be considered is the convergence of the space-frame Eq. (2.6) in the outer region in the basis set (jl) for each value of J and parity. The calculation of the cross section for transitions involving higher rotational states will require the solutions of equations for large values of J . At the same time the number of coupled channels (j, l) will increase [by $\min(J, j) + 1$ for even parity, $(-1)^{J+j+1} = 1$, and by $\min(J, j)$ for odd parity, $(-1)^{J+j+1} = -1$] with the introduction of each new rotational state j . The consideration of higher values of J will also mean that one has to calculate the fixed-nuclei R^λ matrix [Eq. (3.6)] at the boundary point r_t for higher values of λ , since $|\lambda| \leq \min(l, J)$ from Eq. (3.11). In addition to this, because of

TABLE III. Convergence of $\sigma_{0 \rightarrow j}^J$ (\AA^2), calculated from the frame-transformation theory using the pseudopotential, with the number of rotational states coupled in Eq. (2.6) in the outer region: incident electron energy = 1.75 eV, $r_t = 11.774$ a.u., even parity.^a

| J^b | j'_{\max}^c | N_t^d | 0→0 | 0→1 | 0→2 | 0→3 | 0→4 | 0→5 | 0→6 | 0→7 |
|-------|---------------|---------|--------|-------|-------|-------|--------|-------|-------|-------|
| 0 | 2 | 3 | 10.860 | 0.691 | 0.339 | | | | | |
| | 3 | 4 | 10.861 | 0.699 | 0.338 | 0.001 | | | | |
| | 4 | 5 | 10.861 | 0.699 | 0.338 | 0.001 | 0.000 | | | |
| | 5 | 6 | 10.861 | 0.699 | 0.338 | 0.001 | 0.000 | 0.000 | | |
| 1 | 2 | 5 | 0.647 | 5.103 | 1.416 | | | | | |
| | 3 | 7 | 0.959 | 4.547 | 0.678 | 2.142 | | | | |
| | 4 | 9 | 0.959 | 4.546 | 0.679 | 2.141 | 0.000 | | | |
| | 5 | 11 | 0.959 | 4.547 | 0.679 | 2.141 | 0.000 | 0.000 | | |
| 2 | 2 | 6 | 26.872 | 4.209 | 7.471 | | | | | |
| | 3 | 9 | 24.914 | 4.107 | 6.868 | 3.142 | | | | |
| | 4 | 12 | 17.551 | 3.852 | 6.445 | 2.122 | 18.651 | | | |
| | 5 | 15 | 17.547 | 3.850 | 6.441 | 2.138 | 18.636 | 0.001 | | |
| | 6 | 18 | 17.548 | 3.850 | 6.442 | 2.138 | 18.634 | 0.001 | 0.001 | |
| | 7 | 21 | 17.548 | 3.850 | 6.442 | 2.138 | 18.634 | 0.001 | 0.001 | 0.000 |
| 3 | 2 | 6 | 0.059 | 0.018 | 0.029 | | | | | |
| | 3 | 10 | 0.059 | 0.016 | 0.030 | 0.003 | | | | |
| | 4 | 14 | 0.059 | 0.015 | 0.030 | 0.003 | 0.000 | | | |
| | 5 | 18 | 0.059 | 0.011 | 0.033 | 0.003 | 0.000 | 0.001 | | |
| | 6 | 22 | 0.059 | 0.011 | 0.033 | 0.003 | 0.000 | 0.001 | 0.000 | |
| | 7 | 25 | 0.059 | 0.011 | 0.033 | 0.003 | 0.000 | 0.001 | 0.000 | |
| 4 | 2 | 6 | 0.015 | 0.008 | 0.010 | | | | | |
| | 3 | 10 | 0.015 | 0.008 | 0.010 | 0.000 | | | | |
| | 4 | 15 | 0.015 | 0.008 | 0.010 | 0.000 | 0.000 | | | |
| | 5 | 20 | 0.015 | 0.008 | 0.010 | 0.000 | 0.000 | 0.000 | | |
| | 6 | 25 | 0.015 | 0.008 | 0.011 | 0.001 | 0.000 | 0.000 | 0.001 | |
| | 7 | 30 | 0.015 | 0.008 | 0.011 | 0.001 | 0.000 | 0.000 | 0.001 | 0.000 |

^aSee text for the description of these quantities.

^bCross sections for values of J higher than 4 were negligibly small.

^cHighest rotational state (starting from $j' = 0$) coupled in Eq. (2.6).

^dTotal number of coupled channels (jl) in Eq. (2.6).

r^{-2} -type behavior of the electron-dipole interaction potential, the solutions of the lab-frame Eq. (2.6) assume their free-wave asymptotic forms at a large distance (say $r = r_\infty$) from the center of mass of the molecule. In the outer region, therefore, one would have to integrate a large set of coupled equations over a wide range of r ($r_t \leq r \leq r_\infty$). All these factors combined together require large machine size and computational time. Hence the solution of Eq. (2.6) in the outer region in a space frame becomes economically quite prohibitive.

We, therefore, restricted ourselves to the calculation of the cross sections for transitions ($0 \rightarrow j'$) and ($1 \rightarrow j'$). In the present case, unlike for the homonuclear diatomic molecules, final-rotational-state quantum number j' can take both even and odd values. Thus in Eq. (2.6) for each J we coupled only those rotational states which were necessary for the convergence of the partial cross sections $\sigma_{0 \rightarrow j}^J$ and $\sigma_{1 \rightarrow j}^J$ in even and odd parities separately. In Table III, we have tabulated $\sigma_{0 \rightarrow j}^J$ with the coupling of each new rotational states in even parity. (The ground rotational state will not be coupled with the odd-parity channels.) These cross sections corre-

spond to 1.75 eV of the incident electron energy.

We have also looked at the convergence of the partial cross sections $\sigma_{1 \rightarrow j}^J$ both for even and odd parities. In all the cases studied we found that maximum number of rotational states are needed to be coupled in even parity with $J = 2, 3$, and 4. It is probably due to the fact that ${}^2\Pi$ is a resonating state therefore maximum contribution to the cross section will come from the coupling of the $l = 1, 2$, and 3 partial waves. For values of $J = 2, 3$, and 4 the first six or seven rotational states of the molecule can be coupled to these values of the orbital angular momenta.

One will also notice from Table III that the slowest rate of convergence in J is for $j \rightarrow j + 1$ and $j + 2$ transitions. [Actually for electron-impact energies ≤ 0.10 eV as many as 100 values of J were required for $\Delta j = \pm 1$ transitions.] The cross sections for these transitions are directly dominated by contribution(s) coming from the long-range electron dipole (and electron octopole if $j + j' \geq 3$) and the electron-quadrupole interactions, respectively. We also found that, for all incident electron energies, the T^J -matrix elements for $\Delta j = \pm 1$ and 2

transitions for values of J higher than 10, obtained from the FT theory were in good agreement with those calculated from the Born approximation considering merely the V_1, V_2 (only the quadrupole part), and V_3 terms of the interaction potential (4.7). In order to calculate the differential scattering cross section for $j \rightarrow j \pm 1$ and $j + 2$ transitions, we, therefore, replace the exact T^J -matrix elements in Eq. (2.14) for $J > 10$ by the corresponding elements calculated from the Born approximation. This will also mean that one has to calculate the fixed nuclei R^λ matrix at $r = r_t$ only for eleven ($\lambda = 0, \dots, 10$) values of λ .

The differential scattering cross section for a $j \rightarrow j'$ transition can be calculated by recasting Eq. (2.12) in the following form

$$\frac{d\sigma_{j \rightarrow j'}}{d\Omega} = \frac{d^B \sigma_{j \rightarrow j'}}{d\Omega} + \frac{k_j^{-2}}{4(2j+1)} \sum_L [A_L^{(jj')} - {}^B A_L^{(jj')}] \times P_L(\cos\theta). \quad (4.12)$$

In this relation, $d^B \sigma_{j \rightarrow j'}/d\Omega$ is the differential cross section calculated from Born approximation and the coefficients A_L are defined by Eq. (2.13) where maximum value of J in (2.14) is J_{\max} beyond which the exact T^J matrix can be replaced by those calculated from the Born approximation. ${}^B A_L$ is also calculated from Eq. (2.13) by using the Born T^J matrix in Eq. (2.14) up to J_{\max} . (The relevant formulas of Born approximation are given in the Appendix.) Consequently, the scattering and the momentum-transfer cross sections for transitions $j \rightarrow j \pm 1$ and $j + 2$ are calculated from

$$\sigma_{j \rightarrow j'} = {}^B \sigma_{j \rightarrow j'} + \frac{\pi k_j^{-2}}{2j+1} (A_0^{(jj')} - {}^B A_0^{(jj')}) \quad (4.13)$$

and

$$\begin{aligned} \sigma_{j \rightarrow j'}^m = {}^B \sigma_{j \rightarrow j'}^m + \frac{\pi k_j^{-2}}{2j+1} [& (A_0^{(jj')} - \frac{1}{3} A_1^{(jj')}) \\ & - ({}^B A_0^{(jj')} - \frac{1}{3} {}^B A_1^{(jj')})], \end{aligned} \quad (4.14)$$

respectively. ${}^B \sigma_{j \rightarrow j'}$ is the scattering and ${}^B \sigma_{j \rightarrow j'}^m$ the momentum-transfer cross section for ($j \rightarrow j'$) transition calculated from the Born approximation [see Eqs. (A12) and (A13)].

C. Final results

The momentum transfer cross-section inferred from swarm experiments by Hake and Phelps⁹ in the energy range between 10^{-3} to 1.0 eV is shown by curve A in Fig. 2. The dotted curve A' above 1.0 eV, which peaks at about 1.50 eV, was chosen by these experimentalists to extrapolate smoothly to their derived curve A at lower energies.

We have extended the rotational c.c. calculation

of Crawford and Dalgarno¹⁸ in a space-fixed frame of reference to higher energies. The total momentum-transfer cross section $\sigma^m(0)$ obtained from this calculation is marked B in Fig. 2. One finds that the model potential (4.1) of these authors reproduces the momentum-transfer cross section measured by Hake and Phelps⁹ very well up to 0.10 eV. However, when we use this potential for higher incident energies the theoretical results (curve B) begin to deviate from the inferred values (curve A). These computed results also show a very broad peak near 1.50 eV ranging from about 0.60 to 5.0 eV. On the basis of the eigenphase sums obtained by using the potential (4.1) in the fixed-nuclei Eq. (2.22) and shown in Fig. 1, one will conclude that it is probably the combination of ${}^2\Sigma$ and ${}^2\Pi$ resonances which is responsible for this broad peak in curve B (Fig. 2).

The momentum-transfer cross section calculated by an application of our methodology, developed in the preceding sections to $e^- - \text{CO}$ scattering is shown by curve D of Fig. 2. These results are obtained with the renormalized value of the dipole term in the static potential [Eq. (4.10)]. On comparing these new results with those computed from the original V_1 term in the multipole expansion, which are marked C in Fig. 2, we find that rescaling of this term has maximum effect on thermal-energy electron scattering momentum-transfer cross section. The electron-polar-molecule scattering in this energy range is very much dominated by the long-range electron-dipole interaction.⁴² Therefore, a decrease in the magnitude of the dipole moment by ζ_d [Eq. (4.9)] has suppressed the contribution of $\sigma_{0 \rightarrow 1}^m$ to $\sigma^m(0)$ approximately by a factor of ζ_d^2 [see Eq. (A13)]. For higher incident electron energies the dipole potential becomes less important and the short-range forces take up the scattering process. We therefore find that the momentum-transfer cross section calculated with the original dipole-term static potential (curve C) decreases very rapidly with the increasing incident electron velocity and by the time the impact energy becomes 0.10 eV the results of curve C are only 18% higher than those of curve D.

The rescaling of the dipole term has therefore mainly affected the extremely low-energy electron scattering from CO molecule. The small differences in the values of the momentum-transfer cross sections at higher incident electron energies calculated with two different magnitudes of the V_1 term support our argument of Sec. IV B 3 that a rather phenomenological renormalization of only the dipole term in the multipole expansion of the static potential does not have a serious effect on the short-range terms of the electron-CO interaction potential.

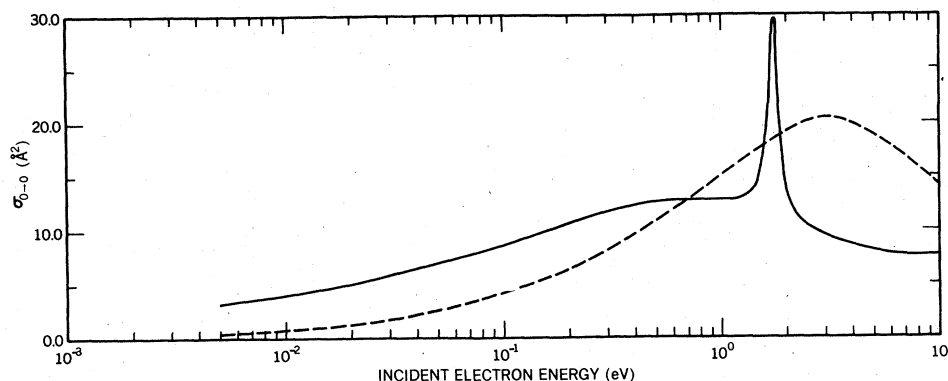


FIG. 4. Elastic scattering cross section for $(0 \rightarrow 0)$ rotational transition. The broken curve was computed by solving the rotational close-coupling Eqs. (2.6) with the model potential (4.1) of Crawford and Dalgarno (Ref. 18). The final results, shown by the continuous curve, were obtained by combining the single-center pseudopotential method with the frame-transformation theory and renormalized dipole term in the static potential.

The new momentum-transfer cross section (curve *D*), on the other hand, is in good agreement with the inferred values⁹ (curve *A*). (Hake and Phelps do not give any error limits for their results in Ref. 9.) Also, the results of curve *D* reproduce the 1.75-eV $^2\Pi$ resonance very well. In addition to this, our calculated momentum-transfer cross section beyond 2 eV is indistinguishable from that of dotted curve *A'* which Hake and Phelps⁹ has obtained by an extrapolation of their inferred results below 1 eV (curve *A*). These extrapolated results have their maximum value around 1.50 eV which is about 0.25 eV lower than the position of the maxima in the calculated curve *D*. Although one can always adjust the resonance position in our pseudopotential method by finding an appropriate value for the parameter r_0 in the polarization potential (4.5) but the magnitude of the cross section, which is about 44% higher than the extrapolated values of curve *A'* in the resonance energy region, is not controlled by any disposable parameter in our calculation. Hake and Phelps⁹ do not discuss the accuracy or reliability of their extrapolated results of the momentum-transfer cross section in this sensitive resonance region. A better comparison in between the theory and experiment will, therefore, require further measurements of the momentum-transfer cross section in this energy domain. However, our computed momentum-transfer cross section, which is obtained by using a single parameter in the polarization potential, is in satisfactory good agreement with the experimental measurements over the whole range of energy. [In addition to the present study of e^- -CO scattering, we have also found in our e^- -N₂ work^{6,10} that the pseudopotential method tends to over estimate the low-energy (<1.00 eV) cross sections; while the agreement between theory and experiment improves significantly in going towards

higher incident energies. A plausible explanation for this behavior of the cross section may be that the present method of treating the exchange and polarization potentials overemphasizes the latter effect for low-energy electron scattering.]

Figure 4 contains the elastic scattering cross section for $(0 \rightarrow 0)$ rotational transition. The continuous curve shows the results which were obtained from an application of the FT theory to the single-center pseudopotential method with renormalized dipole term while the broken curve corresponds to our extension of the rotational c.c. calculation of Crawford and Dalgarno.¹⁸ The pseudopotential results of the continuous curve reproduce the 1.75-eV resonance very well.

The excitation cross section σ_{0-1} calculated from two different potentials have been plotted in Fig. 5. The cross section for $\Delta j = \pm 1$ transitions in a polar molecule will always be large at very low incident electron energies for reasonably large values of dipole moment. A very good agreement between the two curves of Fig. 5 at low energies is in accordance with our contention that the renormalization of the dipole term has improved the asymptotic behavior of the potential without making any significant change in its short-range nature.

The rotational excitation cross sections for $(0 \rightarrow 2)$ and $(0 \rightarrow 3)$ transitions are shown in Fig. 6. [We found that the cross sections obtained from Crawford and Dalgarno potential for transitions higher than $(0 \rightarrow 2)$ were negligibly small.] The σ_{0-2} results calculated from two different potentials are again in good agreement up to 1.0 eV. The cross section for this transition in the low-energy domain will, however, depend upon the quadrupole moment and the nonspherical component (α_2) of the induced dipole polarizability of the target molecule. For CO molecule the value of α_2 is very small [Eq. (4.11)] and it gives rise to an

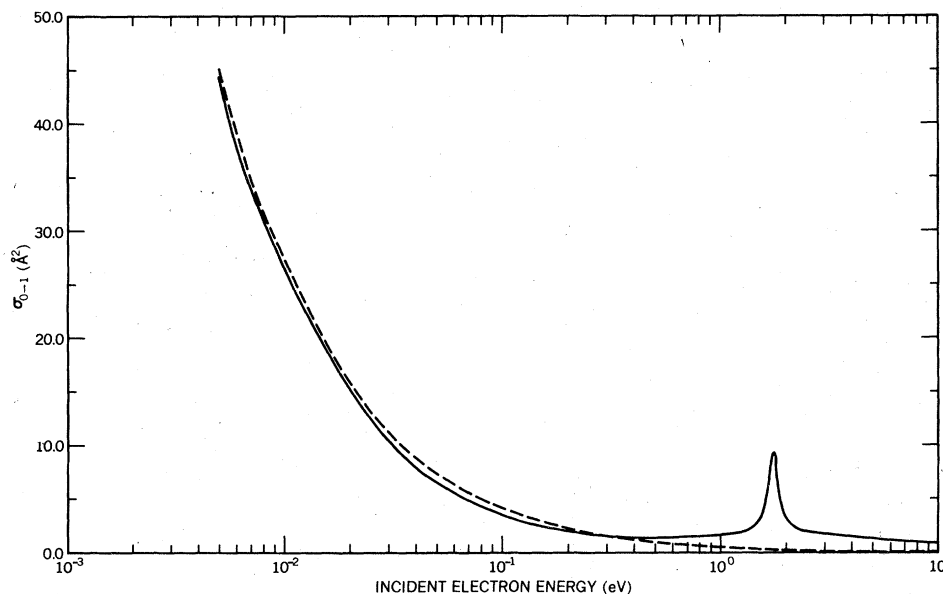


FIG. 5. Same as Fig. 4, but for (0→1) rotational transition.

interaction potential which goes off as r^{-4} [Eq. (4.7)], therefore, it is primarily the electron-quadrupole interaction which will determine the $\sigma_{0 \rightarrow 2}$ cross section for low-energy electrons. As we see from Fig. 6, this interaction gives rise to almost an energy-independent cross section.⁴³ [A difference in the magnitude of the quadrupole moment used in the model potential {Eq. (4.2)} and the pseudopotential {Eq. 4.11} is probably giving rise to a slight difference in the cross sections for (0→2) transition of the broken and continuous curves at these very low energies.] At higher impact energies, however, other short-range terms become important and therefore while the pseudopotential results both for (0→2) and (0→3) transitions go through the resonance but the cross section calculated from the model potential (4.1) does not show this behavior.

The total scattering cross section $\sigma(0)$ is shown in Fig. 7. The good agreement between the broken and the continuous curves at extremely low ener-

gies begins to disappear as the short-range interaction becomes important at higher energies. Although the pseudopotential results have a large spike at 1.75 eV, but those calculated from Crawford and Dalgarno¹⁸ potential (4.1) show a wide resonance-type behavior around 3.00 eV. Also there is a big difference in the maximum values of the cross section obtained from these two different calculations.

A comparison of Figs. 2 and 7 will also reveal that $\sigma^m(0)$ and $\sigma(0)$ calculated from the model potential of Crawford and Dalgarno have their maxima at two different energies, 1.50 and 3.00 eV, respectively. While in the case of the pseudopotential method both of these quantities peak at 1.75 eV, which is the position of the resonance in $^2\Pi$ state of the ($e^- + \text{CO}$) system.³⁶

Such a detailed comparison of the various cross sections computed using these two different potentials in the scattering equations makes two very important points about the nature of these interac-

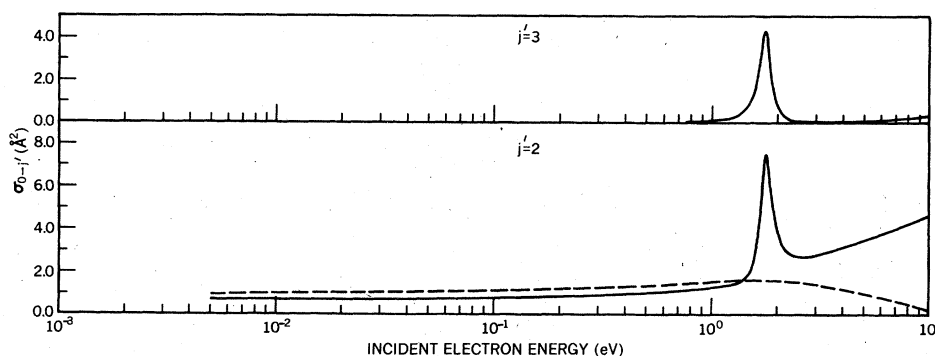


FIG. 6. Same as Fig. 4, but for (0→2) and (0→3) rotational transitions. [The broken curve results for (0→3) transition were negligibly small.]

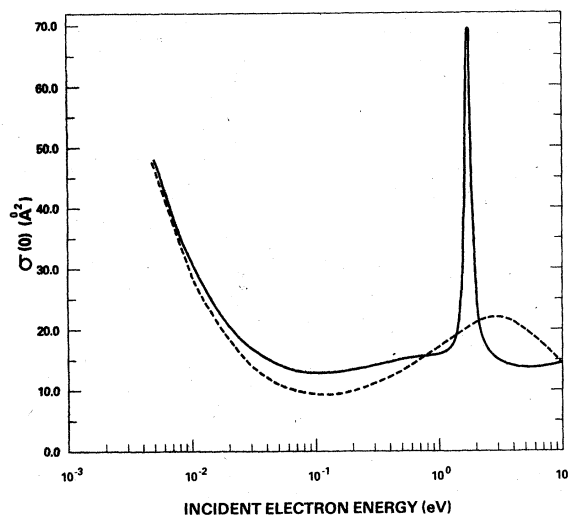


FIG. 7. Total scattering cross section $\sigma(0)$. The broken curve was computed by solving the rotational close-coupling Eq. (2.6) with the model potential (4.1) of Crawford and Dalgarno (Ref. 18). The final results, shown by the continuous curve, were obtained by combining the single-center pseudopotential method with the frame-transformation theory and renormalized dipole term in the static potential.

tions. While the momentum-transfer cross section computed from the pseudopotential is in good agreement with the measurements over the whole energy range, but for thermal electrons, where the scattering is primarily determined by the long-range terms of the interaction potential, the model potential (4.1) gives a better fit to the experimental data. However, as probably anticipated by Crawford and Dalgarno,¹⁸ because this model fails to represent the short-range forces, it should, therefore, not be used to calculate either the low-energy elastic scattering cross sections or to study the e^- -CO scattering at higher energies. Secondly, the renormalization of the dipole term in the multipole expansion of the charge distribution of carbon monoxide used in our pseudopotential method has improved its asymptotic behavior without altering the short-range nature of this potential.

The individual contributions to $\sigma(0)$ and $\sigma^m(0)$ are given in Tables IV and V, respectively. Tables VI and VII contain, on the other hand, rotationally elastic and inelastic scattering cross sections $\sigma_{i \rightarrow j}$, and the momentum-transfer cross sections $\sigma_{i \rightarrow j}^m$, for $j' = 0-5$. In all these tables, both the scattering and the momentum-transfer cross sec-

TABLE IV. Elastic and excitation cross sections^a for $(0 \rightarrow j')$ transitions.

| Incident electron energy E_0 (eV) | σ_{0-0} | σ_{0-1} | σ_{0-2} | σ_{0-3} | σ_{0-4} | $\sigma(0)$ |
|-------------------------------------|----------------|----------------|----------------|----------------|----------------|-------------|
| 0.005 | 3.17 | 44.38 | 0.68 | 0.00 | 0.00 | 48.23 |
| 0.01 | 3.97 | 26.15 | 0.73 | 0.00 | 0.00 | 30.85 |
| 0.03 | 5.77 | 10.47 | 0.75 | 0.00 | 0.00 | 16.99 |
| 0.05 | 6.88 | 6.67 | 0.76 | 0.00 | 0.00 | 14.31 |
| 0.10 | 8.64 | 3.58 | 0.79 | 0.00 | 0.00 | 13.01 |
| 0.60 | 12.66 | 1.52 | 1.07 | 0.03 | 0.00 | 15.28 |
| 1.10 | 12.82 | 1.80 | 1.33 | 0.16 | 0.13 | 16.24 |
| 1.30 | 13.21 | 2.06 | 1.49 | 0.34 | 0.46 | 17.56 |
| 1.50 | 15.37 | 3.00 | 2.02 | 0.94 | 2.19 | 23.52 |
| 1.55 | 16.88 | 3.62 | 2.41 | 1.33 | 3.50 | 27.74 |
| 1.60 | 19.37 | 4.65 | 3.11 | 1.94 | 5.80 | 34.87 |
| 1.65 | 23.28 | 6.31 | 4.35 | 2.87 | 9.76 | 46.57 |
| 1.70 | 27.93 | 8.41 | 6.18 | 3.96 | 15.24 | 61.72 |
| 1.75 | 29.45 | 9.38 | 7.52 | 4.28 | 18.64 | 69.27 |
| 1.80 | 25.69 | 8.12 | 7.15 | 3.38 | 16.59 | 60.93 |
| 1.85 | 20.82 | 6.22 | 5.98 | 2.24 | 12.40 | 47.66 |
| 1.90 | 17.35 | 4.80 | 4.96 | 1.45 | 9.01 | 37.57 |
| 1.95 | 15.18 | 3.90 | 4.25 | 0.96 | 6.74 | 31.03 |
| 2.00 | 13.82 | 3.33 | 3.78 | 0.67 | 5.25 | 26.85 |
| 2.40 | 10.67 | 2.07 | 2.78 | 0.11 | 1.79 | 17.42 |
| 3.00 | 9.57 | 1.78 | 2.79 | 0.05 | 1.08 | 15.27 |
| 4.00 | 8.59 | 1.54 | 3.14 | 0.08 | 0.90 | 14.25 |
| 5.00 | 8.02 | 1.36 | 3.50 | 0.11 | 0.90 | 13.89 |
| 8.00 | 7.59 | 0.97 | 4.27 | 0.18 | 1.07 | 14.08 |
| 10.00 | 7.86 | 0.80 | 4.43 | 0.21 | 1.17 | 14.47 |

^aIn \AA^2 .

TABLE V. Momentum-transfer cross sections^a for (0→j') transitions.

| Incident electron energy E_0 (eV) | $\sigma_{0 \rightarrow 0}^m$ | $\sigma_{0 \rightarrow 1}^m$ | $\sigma_{0 \rightarrow 2}^m$ | $\sigma_{0 \rightarrow 3}^m$ | $\sigma_{0 \rightarrow 4}^m$ | $\sigma^m(0)$ |
|--|------------------------------|------------------------------|------------------------------|------------------------------|------------------------------|---------------|
| 0.005 | 3.50 | 11.04 | 0.68 | 0.00 | 0.00 | 15.22 |
| 0.01 | 4.48 | 5.06 | 0.72 | 0.00 | 0.00 | 10.26 |
| 0.03 | 6.73 | 1.18 | 0.75 | 0.00 | 0.00 | 8.66 |
| 0.05 | 8.13 | 0.50 | 0.77 | 0.00 | 0.00 | 9.40 |
| 0.10 | 10.37 | 0.16 | 0.81 | 0.00 | 0.00 | 11.34 |
| 0.60 | 14.17 | 1.19 | 1.23 | 0.05 | 0.01 | 16.65 |
| 1.10 | 12.93 | 1.99 | 1.70 | 0.22 | 0.13 | 16.97 |
| 1.30 | 12.80 | 2.40 | 2.02 | 0.47 | 0.47 | 18.16 |
| 1.50 | 14.12 | 3.41 | 2.87 | 1.31 | 2.22 | 23.93 |
| 1.55 | 15.17 | 3.97 | 3.39 | 1.84 | 3.53 | 27.90 |
| 1.60 | 16.88 | 4.83 | 4.22 | 2.69 | 5.84 | 34.46 |
| 1.65 | 19.44 | 6.07 | 5.55 | 3.99 | 9.80 | 44.85 |
| 1.70 | 22.12 | 7.35 | 7.21 | 5.50 | 15.27 | 57.45 |
| 1.75 | 22.14 | 7.44 | 7.99 | 5.94 | 18.63 | 62.14 |
| 1.80 | 18.67 | 5.95 | 7.03 | 4.69 | 16.55 | 52.89 |
| 1.85 | 14.96 | 4.36 | 5.58 | 3.11 | 12.35 | 40.36 |
| 1.90 | 12.51 | 3.33 | 4.51 | 2.01 | 8.96 | 31.32 |
| 1.95 | 11.04 | 2.74 | 3.84 | 1.34 | 6.70 | 25.66 |
| 2.00 | 10.13 | 2.40 | 3.43 | 0.93 | 5.21 | 22.10 |
| 2.40 | 7.85 | 1.81 | 2.74 | 0.16 | 1.77 | 14.33 |
| 3.00 | 6.68 | 1.70 | 2.94 | 0.08 | 1.07 | 12.47 |
| 4.00 | 5.56 | 1.52 | 3.45 | 0.12 | 0.90 | 11.55 |
| 5.00 | 4.94 | 1.33 | 3.92 | 0.17 | 0.93 | 11.29 |
| 8.00 | 4.22 | 0.92 | 5.00 | 0.28 | 1.18 | 11.60 |
| 10.00 | 3.97 | 0.77 | 5.38 | 0.32 | 1.33 | 11.77 |

^aIn Å².

tions for $\Delta j = \pm 1$ transitions are largest in the thermal-energy region. These tables also show that all our results for individual transitions reproduce the 1.75-eV ²Π resonance very well. In addition to this, one would also notice that in the resonance energy region—unlike the 0→j' transitions where $\sigma_{0 \rightarrow 4}$ and $\sigma_{0 \rightarrow 4}^m$ have the largest values for excitation cross sections— $\sigma_{1 \rightarrow 3}$ and $\sigma_{1 \rightarrow 3}^m$, although smaller than the elastic $\sigma_{1 \rightarrow 1}$ and $\sigma_{1 \rightarrow 1}^m$, respectively, are maximum among the cross sections for inelastic transitions which start from the first excited rotational state of carbon monoxide. This feature is the same which was found both in the pure rotational excitation^{10,22} and the simultaneous vibration-rotation excitation⁴⁴ in e^- -N₂ scattering.

The differential scattering cross section for (0→j') transitions at 0.01 and 1.50 eV are shown in Fig. 8. The continuous curves represent the pseudopotential (combined with FT theory and the renormalized dipole term) results while the broken curves were computed from the semiempirical potential (4.1) of Ref. 18. [The (0→1) angular distributions at 0.01 eV obtained from these two potentials were indistinguishable on the scale of Fig. 8.] At 1.50 eV the continuous curve for (0→2) transition is no longer isotropic because the short-range interactions in the pseudopotential dominate

the pure quadrupole scattering; while the broken curve is still isotropic.

The definition of the momentum-transfer cross section [Eq. (2.16)] involves a weighting factor of (1 - cosθ) which removes the forward-scattering contributions. A broad peak in the momentum-transfer cross section at 1.50 eV (curve B in Fig. 2) calculated from the semiempirical potential (4.1) is, therefore, exclusively due to the rotationally elastic scattering from CO.

The angular distributions for (0→j') transitions at the resonance energy 1.75 eV, and also at 3.00 eV, are given in Fig. 9. We have computed also the (1→j') differential scattering cross sections from our pseudopotential which are shown in Fig. 10 (at 0.01 and 1.50 eV) and Fig. 11 (at 1.75 and 3.00 eV).

V. CONCLUSION

The work presented here probably constitutes the very first study of electron scattering from such a complex system as carbon monoxide using *ab initio* methods. Although, to check the accuracy of the various cross sections given here more experimental measurements will be required in future but the basic fact that the computed momentum-

TABLE VI. Elastic and inelastic cross sections (in Å²) for (1→j') transitions.

| Incident electron energy ^a E_0 (eV) | σ_{1-0} | σ_{1-1} | σ_{1-2} | σ_{1-3} | σ_{1-4} | σ_{1-5} | $\sigma(1)$ |
|--|----------------|----------------|----------------|----------------|----------------|----------------|-------------|
| 0.005 | 16.35 | 3.33 | 24.94 | 0.32 | 0.00 | 0.00 | 44.94 |
| 0.01 | 9.15 | 4.14 | 15.01 | 0.41 | 0.00 | 0.00 | 28.71 |
| 0.03 | 3.55 | 5.94 | 6.10 | 0.44 | 0.00 | 0.00 | 16.03 |
| 0.05 | 2.24 | 7.06 | 3.90 | 0.45 | 0.00 | 0.00 | 13.65 |
| 0.10 | 1.20 | 8.84 | 2.11 | 0.47 | 0.00 | 0.00 | 12.62 |
| 0.60 | 0.51 | 13.05 | 0.98 | 0.64 | 0.02 | 0.00 | 15.20 |
| 1.10 | 0.60 | 13.34 | 1.24 | 0.85 | 0.09 | 0.07 | 16.19 |
| 1.30 | 0.69 | 13.80 | 1.50 | 1.10 | 0.19 | 0.26 | 17.54 |
| 1.50 | 1.00 | 16.19 | 2.38 | 2.18 | 0.54 | 1.22 | 23.51 |
| 1.55 | 1.21 | 17.86 | 2.96 | 3.00 | 0.76 | 1.95 | 27.74 |
| 1.60 | 1.55 | 20.63 | 3.91 | 4.44 | 1.11 | 3.23 | 34.87 |
| 1.65 | 2.10 | 25.05 | 5.42 | 6.95 | 1.64 | 5.43 | 46.59 |
| 1.70 | 2.80 | 30.43 | 7.29 | 10.48 | 2.26 | 8.48 | 61.74 |
| 1.75 | 3.13 | 32.46 | 8.07 | 12.80 | 2.45 | 10.36 | 69.27 |
| 1.80 | 2.71 | 28.54 | 6.85 | 11.67 | 1.92 | 9.23 | 60.92 |
| 1.85 | 2.07 | 23.18 | 5.09 | 9.10 | 1.27 | 6.90 | 47.61 |
| 1.90 | 1.60 | 19.30 | 3.81 | 6.98 | 0.82 | 5.01 | 37.52 |
| 1.95 | 1.30 | 16.84 | 3.00 | 5.55 | 0.53 | 3.75 | 30.97 |
| 2.00 | 1.11 | 15.32 | 2.49 | 4.59 | 0.42 | 2.91 | 26.84 |
| 2.40 | 0.69 | 11.77 | 1.42 | 2.47 | 0.06 | 1.00 | 17.41 |
| 3.00 | 0.59 | 10.67 | 1.20 | 2.16 | 0.03 | 0.60 | 15.25 |
| 4.00 | 0.51 | 9.84 | 1.06 | 2.29 | 0.05 | 0.50 | 14.25 |
| 5.00 | 0.45 | 9.42 | 0.95 | 2.51 | 0.06 | 0.50 | 13.89 |
| 8.00 | 0.32 | 9.30 | 0.72 | 3.05 | 0.11 | 0.59 | 14.09 |
| 10.00 | 0.27 | 9.64 | 0.62 | 3.17 | 0.12 | 0.64 | 14.46 |

^aThis value (E_0) corresponds to the energy of the electron incident on the ground rotational state of CO. The appropriate energy of incidence for the first rotational state of the molecule can be obtained from the energy conservation law: $E_1 = E_0 - 2B$, $B = 2.38 \times 10^{-4}$ eV for CO molecule.

transfer cross section over the whole energy range is in good agreement with the values inferred from swarm experiments is assuring enough that the other results too should be in satisfactorily good agreement with the future measurements.

As regard to the FT theory, which has formed the basis of the present study, our opinion is that it provides a good formalism for studying the electron-molecule scattering from first principles. The convenience with which the short-range forces can be included by working in a fixed-nuclei approximation in the inner region and at the same time allowing the introduction of nuclear degrees of freedom in the outer region makes this theory quite attractive. We have shown here how our single-center pseudopotential method—combined with the R matrix—can be adapted to the FT theory.

Our experience, however, is that the practical implementation of the FT theory is an extremely arduous task. As we have pointed out elsewhere in this article, it is a multistep process. The absence of a rigorous criterion for the selection of a value for the inner-molecular-core radius, where a transformation from a molecule- to a

space-fixed frame of reference should be performed, introduces an element of uncertainty in its application. In addition to this, considerable effort has to be made in solving the scattering problem in the outer region in a space-fixed frame of reference.

This complexity will increase further when one wants to include both the nuclear vibration and rotation in the outer region. A great disparity in the time period of these motions will now require two different points in the configuration space in order to introduce in the scattering equations the Hamiltonians associated with these two modes of nuclear motion. This in turn will also mean that one has to perform two separate transformations—one each for the vibration and rotation. In spite of the availability of high-speed and large-memory computing machines, it seems to us that one should make a very careful judicious study of the problem at hand before deciding to use the FT theory.

ACKNOWLEDGMENTS

The realization that the frame-transformation theory, combined with the R -matrix method, should

be employed to study electron scattering from polar molecules came about from very long discussions with Professor P. G. Burke. I am very much grateful to Professor Burke for several of his illuminating suggestions in the incipient stages of this work and for supplying his \underline{R} -matrix theory notes. Many useful discussions with Dr. A. Temkin and his continuous encouraging supervision during the course of a very involved calculation has been conducive in bringing this project to a successful end. I am also indebted to other members of the Theoretical Studies Group with whom intermittent discussions have benefited me on several occasions. It would probably not have been possible to finish this calculation without a generous

use of the excellent computing facilities at Goddard Space Flight Center and the cooperation of the computer center personnel.

APPENDIX

The Born-approximation theory of electron-molecule scattering is very well formulated.^{43,45} In this Appendix, we give the relevant formulas and put them in a form directly applicable to the present study.

The $T_{j'l',jl}^J$ matrix element for a transition from the initial rotational state j to the final state j' calculated in Born approximation from a set of coupled scattering Eqs. (2.6) is given by⁴⁶

$${}^B T_{j'l',jl}^J = -2i\pi \sum_{\mu=1}^{\infty} f_{\mu}(j'l',jl;J) \int_0^{\infty} J_{l'+1/2}(k_{j'},r) V_{\mu}(r) J_{l+1/2}(k_j,r) r dr, \quad (\text{A1})$$

where coefficient

$$f_{\mu}(j'l',jl;J) = \langle Y_{j'l'}^J | P_{\mu}(\hat{r} \cdot \hat{R}) | Y_{jl}^J \rangle \\ = (-1)^{-J-\mu} [(2j'+1)(2l'+1)(2j+1)(2l+1)]^{1/2} \begin{pmatrix} j & j' & \mu \\ 0 & 0 & 0 \end{pmatrix} \begin{pmatrix} l & l' & \mu \\ 0 & 0 & 0 \end{pmatrix} \begin{Bmatrix} j & l & J \\ l' & j' & \mu \end{Bmatrix} \quad (\text{A2})$$

TABLE VII. Momentum-transfer cross sections^a for $(1 \rightarrow j')$ transitions.

| Incident electron energy ^b E_0 (eV) | $\sigma_{1 \rightarrow 0}^m$ | $\sigma_{1 \rightarrow 1}^m$ | $\sigma_{1 \rightarrow 2}^m$ | $\sigma_{1 \rightarrow 3}^m$ | $\sigma_{1 \rightarrow 4}^m$ | $\sigma_{1 \rightarrow 5}^m$ | $\sigma^m(1)$ |
|---|------------------------------|------------------------------|------------------------------|------------------------------|------------------------------|------------------------------|---------------|
| 0.005 | 4.07 | 3.64 | 8.10 | 0.32 | 0.00 | 0.00 | 16.13 |
| 0.01 | 1.77 | 4.63 | 3.56 | 0.40 | 0.00 | 0.00 | 10.36 |
| 0.03 | 0.40 | 6.89 | 0.81 | 0.44 | 0.00 | 0.00 | 8.54 |
| 0.05 | 0.17 | 8.31 | 0.34 | 0.45 | 0.00 | 0.00 | 9.27 |
| 0.10 | 0.05 | 10.58 | 0.11 | 0.48 | 0.00 | 0.00 | 11.22 |
| 0.60 | 0.40 | 14.65 | 0.82 | 0.74 | 0.03 | 0.00 | 16.64 |
| 1.10 | 0.66 | 13.62 | 1.42 | 1.08 | 0.13 | 0.07 | 16.98 |
| 1.30 | 0.80 | 13.61 | 1.80 | 1.42 | 0.27 | 0.26 | 18.16 |
| 1.50 | 1.14 | 15.28 | 2.83 | 2.71 | 0.75 | 1.23 | 23.94 |
| 1.55 | 1.32 | 16.54 | 3.44 | 3.60 | 1.05 | 1.96 | 27.91 |
| 1.60 | 1.61 | 18.59 | 4.38 | 5.13 | 1.54 | 3.24 | 34.49 |
| 1.65 | 2.02 | 21.68 | 5.76 | 7.69 | 2.28 | 5.44 | 44.87 |
| 1.70 | 2.45 | 25.02 | 7.27 | 11.12 | 3.14 | 8.49 | 57.49 |
| 1.75 | 2.48 | 25.34 | 7.52 | 13.08 | 3.40 | 10.36 | 62.18 |
| 1.80 | 1.99 | 21.48 | 5.97 | 11.58 | 2.67 | 9.22 | 52.91 |
| 1.85 | 1.46 | 17.19 | 4.22 | 8.84 | 1.77 | 6.88 | 40.36 |
| 1.90 | 1.11 | 14.31 | 3.07 | 6.69 | 1.14 | 5.00 | 31.32 |
| 1.95 | 0.91 | 12.57 | 2.40 | 5.29 | 0.74 | 3.74 | 25.65 |
| 2.00 | 0.80 | 11.51 | 2.00 | 4.36 | 0.58 | 2.90 | 22.15 |
| 2.40 | 0.60 | 8.95 | 1.27 | 2.43 | 0.09 | 0.99 | 14.33 |
| 3.00 | 0.57 | 7.86 | 1.17 | 2.24 | 0.05 | 0.59 | 12.48 |
| 4.00 | 0.51 | 6.94 | 1.06 | 2.46 | 0.07 | 0.50 | 11.54 |
| 5.00 | 0.44 | 6.51 | 0.96 | 2.76 | 0.10 | 0.51 | 11.28 |
| 8.00 | 0.31 | 6.21 | 0.73 | 3.53 | 0.17 | 0.62 | 11.57 |
| 10.00 | 0.26 | 6.12 | 0.65 | 3.80 | 0.18 | 0.69 | 11.70 |

^aIn \AA^2 .

^bSee footnote to Table VI.

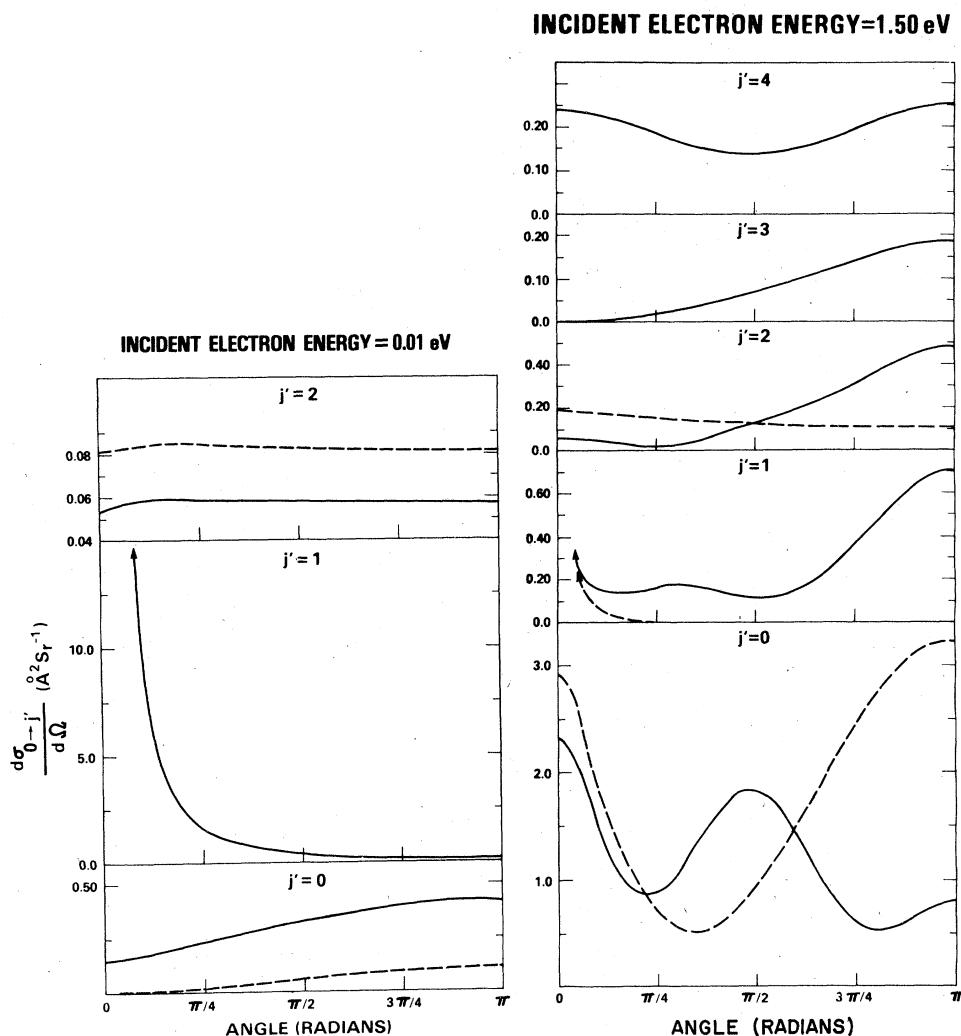


FIG. 8. Differential scattering cross section for $(0 \rightarrow j')$ rotational transitions at 0.01 and 1.50 eV. The broken curves were computed by solving the rotational close-coupling Eqs. (2.6) with the model potential (4.1) of Crawford and Dalgarno (Ref. 18). The final results, shown by the continuous curves, were obtained by combining the single-center pseudopotential method with the frame-transformation theory and the renormalized dipole term in the static potential. [The broken curve results for transitions higher than $(0 \rightarrow 2)$ were negligibly small.]

has already been introduced on the right-hand side of Eq. (2.6). $J_{l+1/2}(x)$ is a Bessel function related to the regular spherical Bessel function of Eq. (3.3) by the following relation

$$J_{l+1/2}(x) = (2x/\pi)^{1/2} j_l(x).$$

If the multipole expansion (2.8) of the electron-molecule electrostatic interaction (2.4) is replaced by its asymptotic form, namely

$$V(\vec{r}; \vec{R}) = \sum_{\mu > 0} \nu_{\mu} r^{-\mu-1} P_{\mu}(\hat{r} \cdot \hat{R}), \quad (\text{A3})$$

where $\nu_1, \nu_2, \nu_3, \dots$, etc. are, respectively, the dipole, quadrupole, octopole, \dots , etc. moments of the molecular charge distribution, the relation (A1) will then become

$${}^B T_{j'l',jl}^j = -2i\pi \sum_{\mu=1}^{\infty} f_{\mu}(j'l',jl;J)\nu_{\mu} \times \int_0^{\infty} J_{l'+1/2}(k_j r) J_{l+1/2}(k_j r) \frac{dr}{r^{\mu}}. \quad (\text{A4})$$

The radial integral (A4) can be evaluated analytically. There are two different cases to be considered:

$$k_j = k_{j'} = k_0 \quad (\text{say}) > 0,$$

$$\int_0^{\infty} J_{l'+1/2}(k_0 r) J_{l+1/2}(k_0 r) \frac{dr}{r^{\mu}} = \frac{k_0^{\mu-1} \Gamma(\mu) \Gamma(S-\mu)}{2^{\mu} \Gamma(S) \Gamma(S-l-\frac{1}{2}) \Gamma(S-l'-\frac{1}{2})} \quad (\mu > 0), \quad (\text{A5})$$

and

$k_j > k_{j'}, > 0$

$$\int_0^\infty J_{l'+1/2}(k_{j'}, r) J_{l+1/2}(k_j, r) \frac{dr}{r^\mu}$$

$$= \frac{k_j^{l'+1/2} \Gamma(S - \mu)}{2^\mu k_j^{l' - \mu + 3/2} \Gamma(l' + \frac{3}{2}) \Gamma(S - l' - \frac{1}{2})}$$

$$\times F\left(S - \mu, l' - S + \frac{3}{2}, l' + \frac{3}{2}; \frac{k_j^2}{k_{j'}^2}\right), \quad \mu > -1, \quad (A6)$$

where we have defined

$$S = \frac{1}{2}(l + l' + \mu) + 1 \quad (A7)$$

and $F(a, b, c; z)$ is a hypergeometric function.⁴⁷

For expressions (A5) and (A6) to be finite the arguments of the Γ functions present in the numerator of these relations should be greater than zero, i.e.,

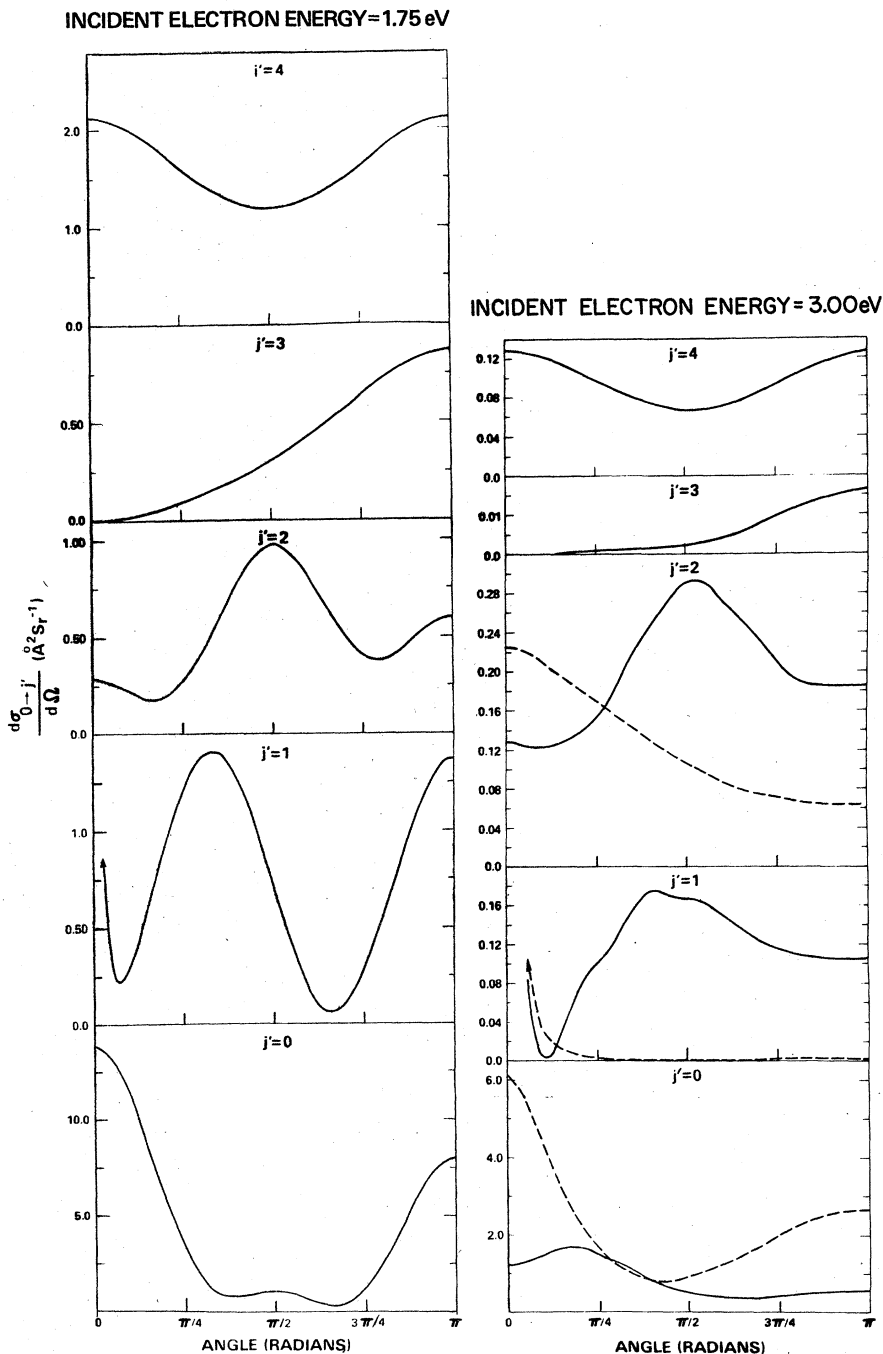


FIG. 9. Same as Fig. 8 for 1.75 and 3.00 eV.

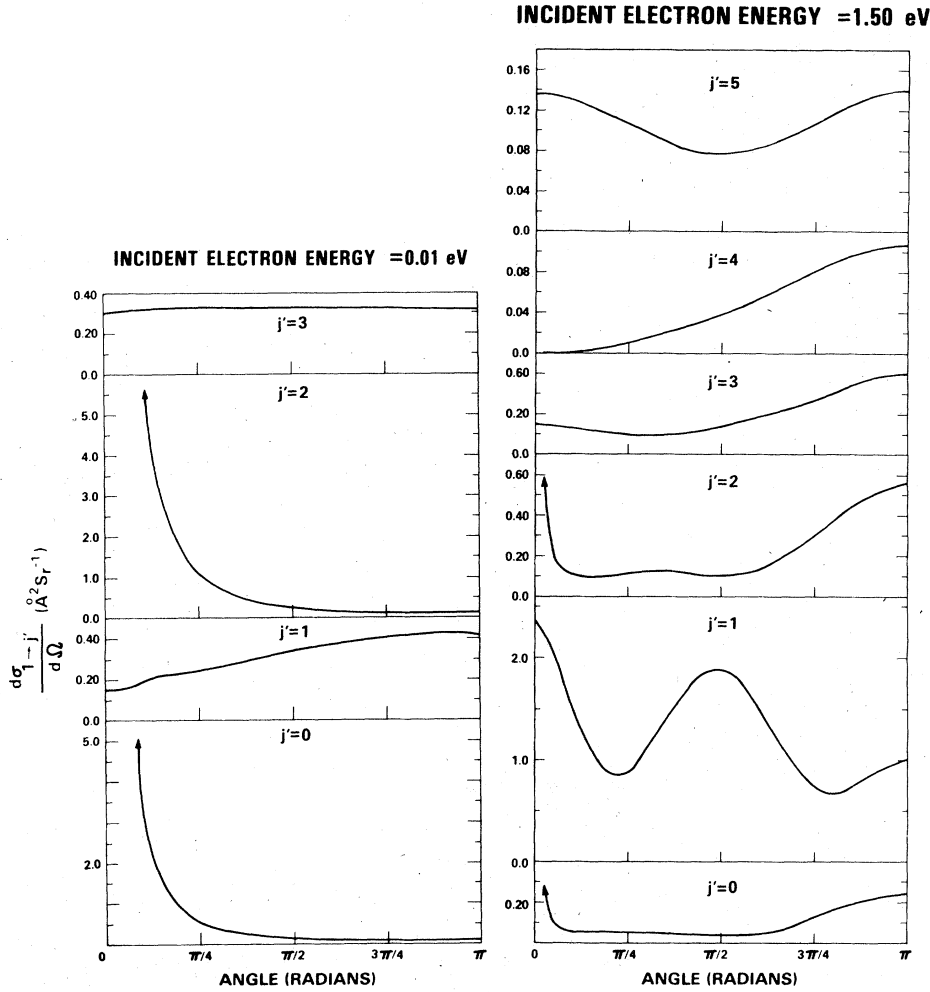


FIG. 10. Differential scattering cross sections for $(1 \rightarrow j')$ rotational transitions at 0.01 and 1.50 eV. These results were obtained by combining the single-center pseudopotential method with the frame-transformation theory and renormalized dipole term in the static potential. Concerning the incident electron energy, see the footnote to Table VI.

$$S - \mu > 0.$$

Or, from (A7),

$$l + l' + 2 > \mu. \quad (\text{A8})$$

The second $3-j$ symbol on the right-hand side of Eq. (A2) will be zero unless $|l - l'| \leq \mu \leq l + l'$. The Born radial integral present in Eq. (A4) will, therefore, always converge as long as the values of l , l' , and μ satisfy the triangular relation $\Delta(l, l', \mu)$. The Born T^J -matrix elements can now be computed by substituting the expression (A5) or (A6), as the case may be, in Eq. (A4). For those values of l , l' , and μ which do not satisfy the inequality (A8), the T^J -matrix element will automatically vanish because of the $3-j$ symbol present in Eq. (A2).

Crawford *et al.*,⁴⁵ have derived an expression for the differential scattering cross section for a $(j \rightarrow j')$ transition. For an electron-molecule interaction of the form (A3), one can write

$$\frac{d^B \sigma_{j-j'}}{d\Omega} = 4(2j'+1) \frac{k_{j'}}{k_j} \sum_{\mu=1}^{\infty} \frac{v_{\mu}^2}{2\mu+1} \begin{pmatrix} j' & j & \mu \\ 0 & 0 & 0 \end{pmatrix}^2 \times \left(\int_0^{\infty} j_{\mu}(Kr) \frac{dr}{r^{\mu-1}} \right)^2, \quad (\text{A9})$$

where \hat{k}_j and $\hat{k}_{j'}$, specify the directions of the initial and final momentum, respectively, and $\vec{K} = \vec{k}_j - \vec{k}_{j'}$, defines the momentum transfer during the collision such that

$$K_{\min} = |k_j - k_{j'}|, \quad K_{\max} = k_j + k_{j'}. \quad (\text{A10})$$

Because

$$\int_0^{\infty} j_{\mu}(Kr) \frac{dr}{r^{\mu-1}} = \frac{\sqrt{\pi} K^{\mu-2}}{2^{\mu} \Gamma(\mu + \frac{1}{2})},$$

the differential scattering cross section is, therefore, given by

$$\frac{d^B \sigma_{j \rightarrow j'}}{d\Omega} = 4\pi(2j'+1) \frac{k_{j'}}{k_j} \sum_{\mu=1} \left[\frac{\nu_{\mu}}{2^{\mu} \Gamma(\mu + \frac{1}{2})} \begin{pmatrix} j & j' & \mu \\ 0 & 0 & 0 \end{pmatrix} \right]^2 \frac{K^{2\mu-4}}{2\mu+1}. \quad (\text{A11})$$

The integrated cross section for an inelastic transition ($j \rightarrow j'$), defined by

$$B_{\sigma_{j \rightarrow j'}} = \int \frac{d^B \sigma_{j \rightarrow j'}}{d\Omega} d\hat{k}_{j'}$$

will now become

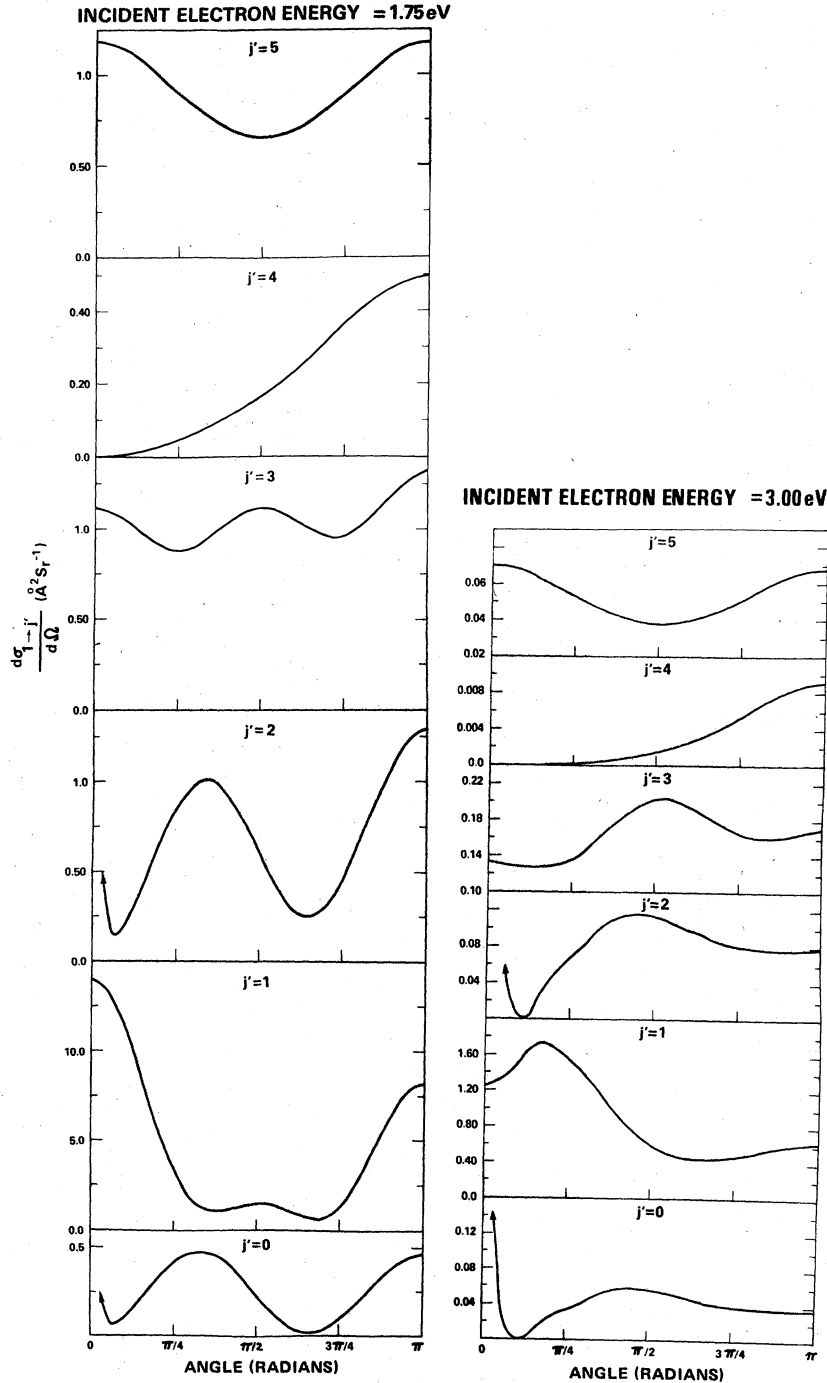


FIG. 11. Same as Fig. 10 for 1.75 and 3.00 eV. Concerning the incident electron energy, see the footnote to Table VI.

$$\begin{aligned}
B_{\sigma_{j \rightarrow j'}} &= \frac{8\pi(2j'+1)}{3k_j^2} D^2 \begin{pmatrix} j & j' & 1 \\ 0 & 0 & 0 \end{pmatrix}^2 \ln \frac{K_{\max}}{K_{\min}} \\
&+ \frac{4\pi^2(2j'+1)}{k_j^2} \sum_{\mu \geq 2} \left[\frac{\nu_\mu}{2^\mu \Gamma(\mu + \frac{1}{2})} \begin{pmatrix} j & j' & \mu \\ 0 & 0 & 0 \end{pmatrix} \right]^2 \\
&\times \frac{K_{\max}^{2\mu-2} - K_{\min}^{2\mu-2}}{(\mu-1)(2\mu+1)},
\end{aligned} \tag{A12}$$

where we have replaced ν_1 by D for the permanent dipole moment of the target molecule. The first term on the right-hand side of Eq. (A12) will obviously be absent for electron scattering from homonuclear diatomic systems.

The momentum-transfer cross section

$$B_{\sigma_{j \rightarrow j'}}^m = \int \frac{d^3 \sigma_{j \rightarrow j'}^m}{d\Omega} (1 - \hat{k}_j \cdot \hat{k}_{j'}) d\hat{k}_j,$$

is given by

$$\begin{aligned}
B_{\sigma_{j \rightarrow j'}}^m &= \frac{8\pi(2j'+1)}{3k_j^2} D^2 \begin{pmatrix} j & j' & 1 \\ 0 & 0 & 0 \end{pmatrix}^2 \left[1 - \frac{K_{\min}^2}{2k_j k_{j'}} \ln \frac{K_{\max}}{K_{\min}} \right] \\
&+ \frac{2\pi^2(2j'+1)}{k_j k_{j'}} \sum_{\mu \geq 2} \left[\frac{\nu_\mu}{2^\mu \Gamma(\mu + \frac{1}{2})} \begin{pmatrix} j & j' & \mu \\ 0 & 0 & 0 \end{pmatrix} \right]^2 \frac{K_{\min}^{2\mu} - K_{\max}^{2\mu} + 4\mu k_j k_{j'} K_{\max}^{2\mu-2}}{(\mu-1)\mu(2\mu+1)}.
\end{aligned} \tag{A13}$$

The K_{\min} and K_{\max} are defined in Eq. (A10) and again the first term on the right-hand side will be present only for electron scattering from polar molecules.

*Work supported in part by a National Academy of Sciences-National Research Council Resident Research Associateship.

†Present address: Physical Research Laboratory, Navrangpura, Ahmedabad-380009, India.

¹N. Chandra, Phys. Rev. A **12**, 2342 (1975).

²For detailed discussions of fixed- and adiabatic-nuclei approximations see, for example, D. E. Golden, N. F. Lane, A. Temkin, and E. Gerjory, Rev. Mod. Phys. **43**, 642 (1971).

³A. M. Arthurs and A. Dalgarno, Proc. R. Soc. A **256**, 540 (1960).

⁴A good compilation of references on this work is given by K. Takayanagi, in *The Physics of Electronic and Atomic Collisions*, edited by J. S. Risley and R. Geballe (University of Washington, Seattle, 1976), pp. 219 ff.

⁵R. J. W. Henry, Phys. Rev. A **2**, 1349 (1970).

⁶N. Chandra and A. Temkin, Phys. Rev. A **13**, 188 (1976).

⁷A. Herzenberg, in *Fundamental Interaction in Physics*, edited by B. Kursunoglu and A. Perlmutter (Plenum, New York, 1973), pp. 261 ff.

⁸E. S. Chang and U. Fano, Phys. Rev. A **6**, 173 (1972).

⁹R. D. Hake and A. V. Phelps, Phys. Rev. **158**, 70 (1967).

¹⁰P. G. Burke and N. Chandra, J. Phys. B **5**, 1696 (1972).

¹¹P. G. Burke, N. Chandra, and F. A. Gianturco, J. Phys. B **5**, 2212 (1972).

¹²N. Chandra and F. A. Gianturco, Chem. Phys. Lett. **24**, 326 (1974).

¹³N. Chandra, Bull. Am. Phys. Soc. **20**, 1470 (1975); *ibid.* **21**, 575 (1976).

¹⁴E. P. Wigner and L. Eisenbud, Phys. Rev. **72**, 29 (1947).

¹⁵R. J. W. Henry and E. S. Chang, Phys. Rev. A **5**, 276 (1972).

¹⁶E. S. Chang, Phys. Rev. Lett. **33**, 1644 (1974).

¹⁷N. Chandra, J. Phys. B **8**, 1953 (1975).

¹⁸O. H. Crawford and A. Dalgarno, J. Phys. B **4**, 494

(1971).

¹⁹M. E. Rose, *Elementary Theory of Angular Momentum* (Wiley, New York, 1957), pp. 49ff.

²⁰M. Rotenberg, R. Bivins, N. Metropolis, and J. K. Wooten, Jr., *The 3-j and 6-j Symbols* (MIT, Cambridge, 1959).

²¹F. H. M. Faisal, J. Phys. B **3**, 636 (1971).

²²N. Chandra, J. Phys. B **8**, 1338 (1975).

²³U. Fano and D. Dill, Phys. Rev. A **6**, 185 (1972).

²⁴P. G. Burke, N. Chandra, and F. A. Gianturco, Mol. Phys. **27**, 1121 (1974).

²⁵M. Born and K. Huang, *Dynamical Theory of Crystal Lattices* (Clarendon, Oxford, 1954), pp. 165 ff.

²⁶A. Temkin and K. V. Vasavada, Phys. Rev. **160**, 109 (1967).

²⁷A. Temkin, K. V. Vasvada, E. Chang, and A. Silver, Phys. Rev. **186**, 57 (1969).

²⁸P. G. Burke and A.-L. Sinfailam, J. Phys. B **3**, 641 (1970).

²⁹A comprehensive review on the R -matrix theory and its application in nuclear physics has been written by A. M. Lane and R. G. Thomas, Rev. Mod. Phys. **30**, 257 (1958).

³⁰For a recent review on the application of the R -matrix method to various electron-atom collision problems, see P. G. Burke and W. D. Robb, Adv. At. Mol. Phys. **11**, 143 (1975).

³¹An approach similar to this for the atomic case has been discussed by P. G. Burke, in *Lectures in Theoretical Physics* (Gordon and Beach, New York), Vol. II C, pp. 34 ff.

³²N. Chandra, Comput. Phys. Commun. **5**, 417 (1973).

³³Here we would like to refer the reader to the footnote given on p. 1342 on Ref. 22 in order to explain the relationship between the transformation (3.11) and the one given earlier by the authors of Ref. 28.

³⁴P. G. Burke, A. Hibbert, and W. D. Robb, J. Phys. B **4**, 153 (1972).

³⁵The T^J matrix of Eqs. (2.14) and (2.15) will include

both even- and odd-parity elements.

- ³⁶J. N. Bardsley, F. Mandl, and A. R. Woods, *Chem. Phys. Lett.* 1, 359 (1967).
- ³⁷F. H. M. Faisal and A. L. V. Tench, *Comput. Phys. Commun.* 2, 261 (1971).
- ³⁸A. D. McLean and M. Yoshimine, *IBM J. Res. Dev. Suppl.* 12, 206 (1967); *J. Chem. Phys.* 46, 3862 (1967).
- ³⁹U. Fano, *Phys. Rev. A* 2, 353 (1970).
- ⁴⁰O. Atabek, D. Dill, and Ch. Jungen, *Phys. Rev. Lett.* 33, 123 (1974).
- ⁴¹M. J. Seaton, *Mon. Not. R. Astron. Soc.* 118, 504 (1958); *Proc. Phys. Soc. Lond.* 88, 801 (1966).
- ⁴²K. Takayanagi, *Comments At. Mol. Phys.* 3, 95 (1972).
- ⁴³K. Takayanagi and Y. Itikawa, *Adv. At. Mol. Phys.* 6, 105 (1970).
- ⁴⁴N. Chandra and A. Temkin, *Phys. Rev. A* 14, 507 (1976).
- ⁴⁵O. H. Crawford, A. Dalgarno, and P. B. Hays, *Mol. Phys.* 13, 181 (1967).
- ⁴⁶M. J. Seaton, *Proc. Phys. Soc.* 77, 174 (1961). Equation (A1) has an additional minus sign because we have $T=S-1$ [see Eq. (2.11)] which is opposite to the definition used by Seaton.
- ⁴⁷M. Abramowitz and I. A. Stegun, *Handbook of Mathematical Functions* (Dover, New York, 1972), pp. 556.